# Final state interactions and the extraction of neutron single spin asymmetries from semi-inclusive deep-inelastic scattering by a transversely polarized $^3$He target

A. Del Dotto,[1] L. P. Kaptari,[2] E. Pace,[3] G. Salmè,[4] and S. Scopetta[5]

[1]*Istituto Nazionale di Fisica Nucleare, Sezione di Roma, Piazzale A. Moro 2, I-00185, Rome, Italy, and University of South Carolina, Columbia, South Carolina 29208, USA*

[2]*Bogoliubov Laboratory of Theoretical Physics, 141980, JINR, Dubna, Russia*

[3]*Physics Department, University of Rome "Tor Vergata" and Istituto Nazionale di Fisica Nucleare, Sezione di Roma Tor Vergata, Via della Ricerca Scientifica 1, I-00133, Rome, Italy*

[4]*Istituto Nazionale di Fisica Nucleare, Sezione di Roma, Piazzale A. Moro 2, I-00185, Rome, Italy*

[5]*Department of Physics and Geology, University of Perugia and Istituto Nazionale di Fisica Nucleare, Sezione di Perugia, Via A. Pascoli, I-06123, Italy*

(Received 13 April 2017; published 12 December 2017)

The semi-inclusive deep-inelastic electron scattering off transversely polarized $^3$He, i.e., the process $e + {}^3\vec{\mathrm{He}} \to e' + h + X$, with $h$ being a detected fast hadron, is studied beyond the plane-wave impulse approximation. To this end, a distorted spin-dependent spectral function of a nucleon inside an $A = 3$ nucleus is actually evaluated through a generalized eikonal approximation, in order to take into account the final state interactions between the hadronizing system and the $(A - 1)$ nucleon spectator one. Our realistic description of both nuclear target and final state is a substantial step forward for achieving a reliable extraction of the Sivers and Collins single spin asymmetries of the free neutron. To illustrate how and to what extent the model dependence due to the treatment of the nuclear effects is under control, we apply our approach to the extraction procedure of the neutron single spin asymmetries from those measured for $^3$He for values of the kinematical variables relevant both for forthcoming experiments at Jefferson Laboratory and, with an exploratory purpose, for the future Electron Ion Collider.

DOI: 10.1103/PhysRevC.96.065203

## I. INTRODUCTION

In recent years, special efforts on both experimental and theoretical sides have been focused on semi-inclusive deep inelastic scattering (SIDIS), i.e., the process $A(l,l'h)X$ where, in the final state, a scattered lepton $l'$ and a hadron $h$ are detected in coincidence, after the interaction of a lepton $l$ with a hadronic system $A$. Nowadays, it is clear that inclusive deep inelastic scattering (DIS), i.e., the process $A(l,l')X$, despite intense experimental investigations in recent decades, cannot answer a few crucial questions on hadron structure. Indeed, at least three long-standing problems cannot be explained through DIS measurements, namely (i) the fully quantitative description of the so-called EMC effect (i.e., the modification of the nucleon partonic structure due to the nuclear medium [1]); (ii) the solution of the so-called "spin crisis," i.e., the fact that the nucleon spin does not originate from only the spins of its valence quarks [2]; (iii) the measurement of the chiral-odd parton distribution function (PDF) called transversity (see, e.g., Refs. [3,4] and references therein quoted) that complements the leading-twist collinear description of a polarized nucleon. As is well known, transversity is related to the amount of transversely polarized quarks inside a transversely polarized nucleon and it is not measurable in DIS, where a flip of the quark chirality cannot take place. Through DIS processes, on both proton (see, e.g., Refs. [5,6]) and nuclear targets (see, e.g., Refs. [7–9]), it is possible to investigate only partonic distributions of longitudinal momentum (i.e., parallel to the direction of the incoming lepton) and helicity. Therefore, in order to access information on the transverse structure of the target, either in coordinate or momentum space, one necessarily has to go beyond DIS measurements (see, e.g., Refs. [10] and [11] for recent reviews on nucleon and nuclear targets, respectively).

SIDIS processes are an important tool for increasing our knowledge of hadron dynamics. Indeed, if the detected hadron is fast, it likely originates from the fragmentation of the active quark, after absorbing the virtual photon. Hence, the detected hadron opens a valuable window on the motion of quarks inside the parent nucleon, before the interaction with the photon occurs. In particular, their transverse motion, not seen in the collinear case, represents the subject of intense experimental efforts in the study of SIDIS reactions, through which one can access the so-called transverse-momentum-dependent parton distributions (TMDs) (see, e.g., Ref. [4]). Those distributions provide a wealth of information on the partonic dynamics, eventually shedding light on the challenging three issues listed above. Besides the main topic represented by TMDs, one should remember that the detected hadron carries also information on the hadronization mechanism itself. The SIDIS cross sections can be parametrized, at leading twist, by six TMDs; this number reduces to three in the collinear case (with only two TMDs measurable in DIS [4]) and increases to eight once the so-called time-reversal odd TMDs (i.e., the Sivers [12] and Boer-Mulders [13] functions) are considered [4].

It should be emphasized that, in order to experimentally investigate the wide field of TMDs, one should measure cross-section asymmetries, using different combinations of beam and target polarizations (see, e.g., Ref. [14]). Moreover, for completing the study of TMDs, one should achieve a sound

 

flavor decomposition, possible only by collecting a detailed knowledge of the neutron TMDs. The present investigation moves from the observation that free neutron targets are not available and nuclei have to be used as effective neutron targets. In particular, the study of the neutron spin structure is highly favored by choosing a polarized $^3$He target, as it has been done extensively in DIS studies. In the 1990s, procedures to extract the neutron spin-dependent structure functions from $^3$He data in the DIS regime, taking properly into account Fermi motion and binding effects, were proposed [15] and successfully applied (see, e.g., Ref. [16]). Such a detailed description of the target nucleus was obtained in plane-wave impulse approximation (PWIA) by using the so-called spin-dependent spectral function, whose diagonal elements yield the probability distribution to find a nucleon with a given momentum, missing energy, and polarization inside the nucleus. It is worth noting that, within PWIA, accurate $^3$He spin-dependent spectral functions, based on realistic calculations of both the target nucleus and the spectator pair in the final state (fully interacting through the $NN$ interaction adopted for $^3$He), have been built and used in the past 20 years [17–22].

The question whether similar procedures can be extended to SIDIS is of great relevance, due to the several experiments that exploit a polarized $^3$He target (see, e.g., Ref. [23]), for accessing the transverse momentum and spin of the partons inside the neutron. For instance, wide interest has arisen about the possibility to use a transversely polarized $^3$He target for measuring azimuthal single spin asymmetries (SSAs) of the neutron, which are sensitive to time-reversal odd TMDs and to the Collins fragmentation functions (FF) [24] generated by leading twist final state interactions [25]. In the first measurements of SSAs, through SIDIS off transversely polarized proton and deuteron targets, the proton SSAs were found to be sizable [26], while those of deuteron were found to be negligible [27], pointing to a large cancellation between the proton and neutron contributions. A high luminosity environment coupled to a suitable neutron target, as a polarized $^3$He (at level of 90%, an effective neutron target), allows one first to better assess the flavor separation and then accurately test its sensitivity to quark angular momenta. Because of the need for increasing experimental knowledge on neutron TMDs through independent measurement, an experiment of SIDIS off transversely polarized $^3$He was soon proposed [28]. As is well known, some significant steps have been already carried out along the suggested path, since azimuthal asymmetries in the production of leading $\pi^{\pm}$ ($K^{\pm}$) from transversely polarized $^3$He have been already measured at Jefferson Laboratory (JLab), with a beam energy of 6 GeV [29], and new experiments will be soon performed after completing the 12-GeV upgrade [30].

In view of those experimental efforts, a realistic PWIA analysis of SIDIS off transversely polarized $^3$He has been performed [31]. A realistic spin-dependent spectral function, corresponding to the nucleon-nucleon AV18 interaction [32], has been used for the description of nuclear dynamics and the issue of the extraction of the neutron information from $^3$He data has been addressed. According to Ref. [31], one can safely extend this to SIDIS, where both PDFs and FFs are involved, as the model-independent extraction procedure is based on the realistic evaluation of the proton and neutron polarizations in $^3$He and widely used in inclusive DIS [16]. As a matter of fact, such an extraction procedure is able to take into account effectively the momentum and energy distributions of the polarized bound nucleons in $^3$He.

In general, SIDIS off nuclear targets can happen through at least two, rather different, sets of processes:

(1) The *standard* reaction (most familiar), where a fast hadron is detected mainly in the forward direction, implying that the hadron has been produced by the leading quark. Therefore, this reaction, representing the dominant mechanism in the kinematics of the JLab experiments of Refs. [29,30], can be used to investigate TMDs inside the hit nucleon.
(2) The *spectator* SIDIS, where a slow $(A-1)$ nucleon system, acting as a spectator of the photon-nucleon interaction, is detected, while the produced fast hadron is not.

The spectator SIDIS process has been proven very useful to investigate the unpolarized DIS functions $F_{1,2}(x)$ of a bound nucleon, and therefore to clarify the origin of the EMC effect (see, e.g., Refs. [33–37]). At the same time, this process can also provide useful information on quark hadronization in a medium, complementary to that obtained so far by the standard SIDIS process. It is noteworthy that the polarization degrees of freedom of the target substantially enrich the wealth of information one can gather, as shown in Ref. [38], where a spectator SIDIS, with a detected deuteron, off a polarized $^3$He target was studied. Through such a polarized SIDIS, one can obtain fresh information on the spin-dependent structure functions $g_{1,2}(x)$ for bound nucleons and, ultimately, on the origin of the polarized EMC effect.

In polarized (as well as unpolarized) SIDIS processes, the effects of the final state interaction (FSI) that occur among the hadronizing system (produced after the quark-photon knockout) and the $(A-1)$ spectator system has to be carefully analyzed. For the case of a polarized $^3$He, this study started in Ref. [38], where the trinucleon *distorted spin-dependent spectral function* has been introduced but restricted to the deuteron spectator system. In order to realistically take into account the abovementioned FSI, a generalized eikonal approximation (GEA) has been adopted, i.e., a framework successfully introduced for describing unpolarized SIDIS off nuclei [33]. To apply such a *distorted spin-dependent spectral function* to the standard polarized SIDIS by $^3\vec{\mathrm{He}}$, one has to consider *all the possible states* of the two-nucleon spectator system. But due to FSI between the spectator system and the quark debris, produced after DIS off an internal nucleon with given polarization, this distribution function is remarkably more complicated than the PWIA spin-dependent spectral function, adopted in the description of both DIS by unpolarized $^3$He [15] and SIDIS [31]. However, efforts for evaluating a realistic *distorted spin-dependent spectral function* are worth attempting since its thorough knowledge represents a fundamental help for reliably disentangling TMDs from the nuclear structure, in the experimental cross sections. In perspective, an experimental check of the robustness of

the description of the nuclear effects could be in principle carried out by exploiting the isodoublet nature of the trinucleon bound states. In the case of a polarized $^3$H, one could extract (i) the proton polarized structure functions when a spectator SIDIS is considered or (ii) the relevant TMDs when a standard SIDIS is investigated. The proton information extracted from $^3$H could be compared with the ones gathered using free proton targets, shedding light on the relevance and nature of nuclear effects. Nowadays, the use of a polarized $^3$H target seems too challenging, but it is worth mentioning that important achievements have been obtained in the past decade in handling such a problematic target, as demonstrated by the final approval (with scientific rating A), at JLab, of an experiment dedicated to DIS by a $^3$H target [39].

As a concluding remark, it should be pointed out that, at the present stage, the needed relativistic description of SIDIS is restricted to the kinematics and the elementary cross section, as discussed in the following sections. Indeed, in order to embed the very successful nonrelativistic phenomenology of the nuclear structure, developed over the past decades, in a fully Poincaré covariant approach, one could exploit the light-front framework, that originates from the seminal work by Dirac on the forms of relativistic Hamiltonian dynamics [40]. A thorough formal investigation of a light-front spin-dependent spectral function for a $J = 1/2$ target, in impulse approximation, has been recently presented in Ref. [41] (see also Refs. [42,43] for preliminary results). Obviously, this distribution function is the first step for constructing a Poincaré covariant description of SIDIS reactions, since in analogy with the transition from the PWIA spectral function to the distorted one, FSI effects have to be taken into account also in the Poincaré covariant approach.

Aims of the present paper are first to extend the calculation of the distorted spin-dependent spectral function of $^3$He performed in Ref. [38], in order to include the excited states of the two-nucleon spectator system (recall that in Ref. [38] only the deuteron state was retained). As a second step, we apply our formalism to the *standard* SIDIS process, with kinematical conditions typical of experiments to be performed in the next years at JLab and in the future (possibly near) at the Electron Ion Collider (EIC), focusing on the extraction of quark TMDs inside the neutron, i.e., the needed ingredients for making complete the flavor decomposition. One can easily realize that, since in standard SIDIS the final fast hadronic state can reinteract with a two-nucleon scattering state, this process is much more involved than spectator SIDIS, where FSIs occur between the final hadronic state and the detected deuteron.

The paper is organized as follows. In Sec. II, we present the basic formalism for the cross section, valid for the standard SIDIS process, where a hadron $h$ is detected in coincidence with the scattered charged lepton. The main quantities relevant for the calculations are presented and the PWIA framework is reviewed, to better appreciate the difference with the FSI case, discussed in the next sections. In Sec. III, the SIDIS reaction $^3\vec{\text{He}}(e,e'h)X$ is investigated in detail, introducing the distorted spin-dependent spectral function, that represents the main ingredient of our method for implementing FSI effects, through a generalized eikonal approximation. In Sec. IV, the dependence of the nuclear hadronic tensor upon the target polarization is studied. In Sec. V, the expressions to be used for evaluating the nuclear SSAs, both in PWIA and with FSI taken into account, are presented and a strategy for the extraction of the neutron information is discussed. In Sec. VI, the results for the distorted spectral functions and light-cone momentum distributions are presented and compared with the corresponding PWIA calculations; furthermore, the finite values of the momentum and energy transfers corresponding to the actually proposed experiments are adopted for the evaluation of the $^3$He Collins and Sivers asymmetries and for the extraction of neutron asymmetries with FSI effects taken into account and implementing the comparison with the PWIA calculations. Eventually, in the last section, conclusions are drawn and perspectives presented. Important formal details are collected in two appendixes.

## II. THE SIDIS CROSS SECTION

The differential cross section for the generic SIDIS process off a polarized target $A$, i.e., $l + \vec{A} = l' + h + X$ when the final pseudoscalar hadron $h$ is detected, can be written in the laboratory frame and in one-photon exchange approximation as follows (cf., e.g., Refs. [4,34,38]),

$$\frac{d\sigma}{d\varphi_\ell dx_{Bj} dy d\mathbf{P}_h} = \frac{\alpha_{em}^2}{Q^4}\frac{m_N}{2E_h}\, y\, L^{\mu\nu} W_{\mu\nu}^{s.i.}(\mathbf{S}_A, Q^2, P_h), \tag{1}$$

where, for incoming and outgoing charged leptons with 4-momentum $k^\mu = (\mathcal{E},\vec{k})$ and $k'^\mu = (\mathcal{E}',\vec{k}')$, one has $Q^2 = -q^2 = -(k-k')^2 = \vec{q}^{\,2} - \nu^2 = 4\mathcal{E}\mathcal{E}'\sin^2(\theta_\ell/2)$, i.e., the square 4-momentum transfer in ultrarelativistic approximation (with $\vec{q} = \vec{k} - \vec{k}'$, $\nu = \mathcal{E} - \mathcal{E}'$, and $\theta_\ell \equiv \theta_{\widehat{\vec{k}\vec{k}'}}$). Moreover, $x_{Bj} = Q^2/(2m_N\nu)$ is the Bjorken scaling variable, $y = \nu/\mathcal{E}$, $m_N$ is the nucleon mass, $\alpha_{em}$ is the electromagnetic fine structure constant, $\varphi_\ell$ is the azimuthal angle of the detected charged lepton, $P_h = (E_h,\mathbf{P_h})$ is the 4-momentum of the detected hadron $h$ with mass $m_h$, and $\mathbf{S}_A$ is the polarization vector of the target nucleus.

The unpolarized leptonic tensor $L_{\mu\nu}$ is an exactly calculable quantity in QED. In the ultrarelativistic limit it gets the form

$$L_{\mu\nu} = 2[k_\mu k'_\nu + k'_\mu k_\nu - (k\cdot k')g_{\mu\nu}]. \tag{2}$$

The semi-inclusive (s.i.) hadronic tensor of the target with polarization four-vector $S_A$ and mass $M_A^2 = P_A^2$ is defined as

$$\begin{aligned} W_{\mu\nu}^{s.i.}(\mathbf{S}_A, Q^2, P_h) = \frac{1}{2M_A}\sum_X \langle\, S_A, P_A|\hat{J}_\mu|P_h, X\,\rangle \\ \times \langle\, P_h, X|\hat{J}_\nu|S_A, P_A\,\rangle \\ \times \delta^4(P_A + q - P_X - P_h) d\tau_X, \end{aligned} \tag{3}$$

where the covariant normalization $\langle\, p|p'\,\rangle = 2E(2\pi)^3\delta(\mathbf{p}-\mathbf{p}')$ has been assumed and $d\tau_X$ is the suitable phase-space factor for the undetected state $X$, given in turn by a state $X'$ with baryon number 1 and an $A-1$ recoiling nuclear system. One should notice that, in Eq. (3), the integration over the phase-space volume of the detected hadron, $h$, does not have to be performed.

In the following, the cross section for SIDIS off transversely polarized $^3$He will be worked out, taking into account final state interaction effects. For this, it is necessary first to recall the results obtained in PWIA.

Within PWIA, the nuclear tensor Eq. (3) is approximated using the following assumptions: (i) the nuclear current operator is written as the sum of single nucleon operators $\hat{j}^N_\mu$; (ii) the FSI between the debris originating by the struck nucleon and the fully interacting $(A-1)$ nuclear system is disregarded, as suggested by the kinematics of the process under investigation; (iii) the coupling of the virtual photon with the $(A-1)$ system is disregarded, due to the large 4-momentum transferred in the process; (iv) the effect of boosts is not considered (they will be properly taken into account in a light-front framework elsewhere, following the procedure addressed in Refs. [41–43]). In this way, the complicated final baryon states $|P_h, X\rangle$ are approximated by a tensor product of hadronic states, viz.,

$$|P_h, X\rangle^{\rm PWIA} = |P_{A-1}\rangle \otimes |P_h\rangle \otimes |X'\rangle, \tag{4}$$

where $|P_{A-1}\rangle$ indicates the state (properly antisymmetrized) of the fully interacting $(A-1)$-nucleon system, which acts merely as a spectator, $|X'\rangle$ describes the baryonic state that originates together with $|P_h\rangle$ from the hadronization of both the quark which has absorbed the virtual photon and the other colored remnants. The nuclear tensor $W^{s.i.}_{\mu\nu}(\mathbf{S}_A, Q^2, P_h)$ can be related therefore to the one of a single nucleon. This is obtained inserting in Eq. (3) complete sets of nucleon plane waves and $(A-1)$-nucleon interacting states, given by

$$\sum_\lambda \int \frac{d\mathbf{p}_N}{2E_N(2\pi)^3} |\lambda, p_N\rangle\langle \lambda, p_N| = 1, \tag{5}$$

$$\sum_{f_{A-1}} \!\!\!\!\!\!\int_{\epsilon^*_{A-1}} \rho(\epsilon^*_{A-1}) \int \frac{d\mathbf{P}_{A-1}}{2E_{A-1}(2\pi)^3} \times \left|\Phi^{f_{A-1}}_{\epsilon^*_{A-1}}, \mathbf{P}_{A-1}\right\rangle\!\left\langle \Phi^{f_{A-1}}_{\epsilon^*_{A-1}}, \mathbf{P}_{A-1}\right| = 1, \tag{6}$$

where $p_N \equiv \{E_N = \sqrt{m_N^2 + |\mathbf{p}_N|^2}, \mathbf{p}_N\}$ is the on-shell four-momentum of a nucleon and $\Phi^{f_{A-1}}_{\epsilon^*_{A-1}}$ is the intrinsic part of the $(A-1)$-nucleon state with quantum numbers $f_{A-1}$ and energy eigenvalue $\epsilon^*_{A-1}$. Moreover, $E_{A-1} = \sqrt{(M^*_{A-1})^2 + |\mathbf{P}_{A-1}|^2}$ with $M^*_{A-1} = Z_{A-1} m_p + (A-1-Z_{A-1}) m_n + \epsilon^*_{A-1}$. The symbol with the sum overlapping the integral indicates that the $(A-1)$ system has both discrete and continuum energy spectra: This corresponds to negative and positive values of the eigenvalue $\epsilon^*_{A-1}$. In Eq. (6), $\rho(\epsilon^*_{A-1})$ is the proper state density, that for $A = 3$ reads

$$\rho_{2bbu} = \frac{1}{(2\pi)^3}, \quad \rho_{3bbu} = \frac{1}{(2\pi)^6} \frac{m_N \sqrt{m_N \epsilon^*_2}}{2}, \tag{7}$$

with the labels $2bbu$ and $3bbu$ indicating the two-body and three-body breakup channels, respectively. Furthermore, recalling that Eq. (4) implies

$$\sum_X d\tau_X \to \sum_{X'} d\tau_{X'} \sum_{f_{A-1}} \!\!\!\!\!\!\int_{\epsilon^*_{A-1}} \rho(\epsilon^*_{A-1}) \int \frac{d\mathbf{P}_{A-1}}{2E_{A-1}(2\pi)^3}, \tag{8}$$

one obtains the following expression for the nuclear tensor in PWIA:

$$W^{s.i.;IA}_{\mu\nu}(\mathbf{S}_A, Q^2, P_h) = \sum_{X',\lambda\lambda'} \sum_N \int dE\, P^{N\mathbf{S}_A}_{\lambda\lambda'}(E, \mathbf{p}_N) \frac{1}{2E_N} \langle \lambda', p_N | \hat{j}^N_\mu | P_h, X'\rangle \times \langle P_h, X' | \hat{j}^N_\nu | \lambda, p_N \rangle \delta^4(P_A + q - P_{A-1} - P_h - P_{X'}) \times d\tau_{X'} \frac{d\mathbf{P}_{A-1}}{(2\pi)^3}, \tag{9}$$

where, with regard to Eq. (3), $P_{X'} + P_{A-1}$ is in place of $P_X$, and the nucleon three-momentum, $\mathbf{p}_N = \mathbf{P}_A - \mathbf{P}_{A-1}$, is fixed by the translation invariance of the initial nuclear vertex, viz.,

$$\left\langle \Phi^{*\,f_{A-1}}_{\epsilon_{A-1}}, \mathbf{P}_{A-1}; \lambda, p_N \middle| \mathbf{S}_A, P_A \right\rangle = \sqrt{2E_N 2E_{A-1} 2M_A}(2\pi)^3 \delta(\mathbf{P}_A - \mathbf{P}_{A-1} - \mathbf{p}_N) \times \left\langle \Phi^{*\,f_{A-1}}_{\epsilon_{A-1}}; \lambda, \mathbf{p}_N \middle| \mathbf{S}_A, \Phi_A \right\rangle. \tag{10}$$

In Eq. (10), $\Phi_A$ is the intrinsic wave function of the target nucleus, with mass $M_A$ and $(P_A - P_{A-1})^2 \neq m_N^2$.

The matrix elements $P^{N\mathbf{S}_A}_{\lambda\lambda'}(E, \mathbf{p}_N)$ in Eq. (9) contain the description of the nuclear structure and are given in PWIA by

$$P^{N\mathbf{S}_A}_{\lambda\lambda'}(E, \mathbf{p}_N) = \sum_{f_{A-1}} \!\!\!\!\!\!\int_{\epsilon^*_{A-1}} \rho(\epsilon^*_{A-1}) \mathcal{O}^{N\mathbf{S}_A}_{\lambda\lambda'}(\epsilon^*_{A-1}, \mathbf{p}_N) \times \delta(E + M_A - m_N - M^*_{A-1}), \tag{11}$$

where $E$ is the usual missing or removal energy, $E = M^*_{A-1} + m_N - M_A = \epsilon^*_{A-1} + B_A$, with $B_A$ being the binding energy of the target nucleus. The quantity $m_N - E$ is the off-shell mass of a nucleon inside the target nucleus, when the $(A-1)$ system acts as a spectator. In Eq. (11), $\mathcal{O}^{N\mathbf{S}_A}_{\lambda\lambda'}(\epsilon^*_{A-1}, \mathbf{p}_N)$ is the following product of PWIA overlaps

$$\mathcal{O}^{N\mathbf{S}_A}_{\lambda\lambda'}(\epsilon^*_{A-1}, \mathbf{p}_N) = \left\langle \Phi^{f_{A-1}}_{\epsilon^*_{A-1}}, \lambda, \mathbf{p}_N \middle| \mathbf{S}_A, \Phi_A \right\rangle \times \left\langle \mathbf{S}_A, \Phi_A \middle| \Phi^{f_{A-1}}_{\epsilon^*_{A-1}}, \lambda', \mathbf{p}_N \right\rangle. \tag{12}$$

The quantities $P^{N\mathbf{S}_A}_{\lambda\lambda'}(E, \mathbf{p}_N)$, Eq. (11), are the matrix elements of the $2 \otimes 2$ spin-dependent spectral function of a nucleon inside the nucleus $A$, with polarization $\mathbf{S}_A$ [19]. The trace of the spectral function yields the probability distribution to find a nucleon in the nucleus $A$ with three-momentum $\mathbf{p}_N$, removal energy $E$, and spin projection equal to $\lambda$. The suitable normalization is

$$\frac{1}{2} \sum_{\lambda N} \int dE \int d\mathbf{p}_N P^{N\mathbf{S}_A}_{\lambda\lambda}(E, \mathbf{p}_N) = 1. \tag{13}$$

Assuming the polarized target in a pure state, the nuclear wave function has definite spin projections on the spin quantization axis, chosen as usual along the polarization vector $\mathbf{S}_A$. In agreement with the definition of the spin-dependent spectral function given in Refs. [18,19], in the complete set of the nucleon plane waves, the spin projection $\lambda$ and $\lambda'$ are defined with respect to the $z$ axis.

In Ref. [15], the so-called longitudinal spectral function was introduced:

$$P^{N\,||}(E,\mathbf{p}_N) = P^{N\,\mathbf{S}_{||}}_{\frac{1}{2}\,\frac{1}{2}}(E,\mathbf{p}_N) - P^{N\,\mathbf{S}_{||}}_{-\frac{1}{2}-\frac{1}{2}}(E,\mathbf{p}_N), \quad (14)$$

giving the probability distribution to have a nucleon $N$ polarized along the $z$ direction minus the probability distribution to have a nucleon $N$ polarized in the opposite direction to the $z$ axis, if $\mathbf{S}_A = \mathbf{S}_{||}$ is directed along the positive $z$ axis.

In Ref. [31], the spin projections $\lambda$ and $\lambda'$ have been defined with respect to the $x$ axis and the perpendicular spectral function has been defined,

$$P^{N\,\perp}(E,\mathbf{p}_N) = P^{N\,\mathbf{S}_{\perp}}_{\frac{1}{2}\,\frac{1}{2}}(E,\mathbf{p}_N) - P^{N\,\mathbf{S}_{\perp}}_{-\frac{1}{2}-\frac{1}{2}}(E,\mathbf{p}_N), \quad (15)$$

giving the probability distribution to have a nucleon $N$ polarized along the $x$ direction minus the probability distribution to have a nucleon $N$ polarized in the opposite direction to the $x$ axis, if $\mathbf{S}_A = \mathbf{S}_{\perp}$ is directed along the positive $x$ axis. It is worthwhile to note that, due to rotational invariance, the two quantities Eqs. (14) and (15) are equal. In relativistic light-front dynamics, where transverse rotations are interaction dependent, this is not true any more, as has been shown in Ref. [43].

As for the Cartesian coordinates, we adopt the DIS convention, i.e., the $z$ axis is directed along the three-momentum transfer $\mathbf{q}$ and the plane $(x,z)$ is the scattering plane. Notice that, in the DIS limit, the direction of the three-momentum transfer coincides with that of the lepton beam, i.e., $\mathbf{q} \,||\, \mathbf{k}_e$.

The nuclear tensor Eq. (9) can be written

$$W^{s.i.;IA}_{\mu\nu}(\mathbf{S}_A,Q^2,P_h) = \sum_{\lambda\lambda'}\sum_{N}\int d\mathbf{p}_N \int dE \frac{m_N}{E_N} w^{N\,s.i.}_{\mu\nu} \times (\tilde{p}_N,P_h,\lambda'\lambda) P^{N\,\mathbf{S}_A}_{\lambda\lambda'}(E,\mathbf{p}_N), \quad (16)$$

where the integration over $\mathbf{P}_{A-1}$ has been changed to the one over $\mathbf{p}_N = \mathbf{P}_A - \mathbf{P}_{A-1}$, and the semi-inclusive nucleon tensor [cf. Eq. (3)] is given by

$$w^{N\,s.i.}_{\mu\nu}(\tilde{p}_N,P_h,\lambda'\lambda) = \frac{1}{2m_N}\sum_{X'}\langle\, p_N,\lambda'|\hat{j}^N_\mu|P_h,X'\,\rangle\langle\, P_h,X'|\hat{j}^N_\nu|p_N,\lambda\,\rangle \times \delta^4(\tilde{p}_N + q - P_h - P_{X'})d\tau_{X'}, \quad (17)$$

where $\tilde{p}_N = P_A - P_{A-1}$ is such that $\tilde{p}^2_N \neq m^2_N = p^2_N$.

Eventually, for the nuclear cross section given in Eq. (1), $\sigma_A(\mathbf{S}_A) \equiv \dfrac{d\sigma(\mathbf{S}_A)}{d\varphi_\ell dx_{Bj} dy d\mathbf{P}_h}$, one gets the following expression in PWIA:

$$\sigma^{A;IA}(\mathbf{S}_A) = \sum_{\lambda\lambda'}\sum_{N}\int d\mathbf{p}_N \int dE \frac{\tilde{\alpha} m_N}{E_N}\sigma^N_{\lambda\lambda'} P^{N\,\mathbf{S}_A}_{\lambda\lambda'}(E,\mathbf{p}_N), \quad (18)$$

where

$$\sigma^N_{\lambda\lambda'} \equiv \frac{d\sigma^N_{\lambda\lambda'}}{d\varphi_\ell dx_{Bj} dy d\mathbf{P}_h} = \frac{\alpha^2_{em}}{Q^4}\frac{m_N}{(p_N\cdot k)}\frac{m_N\nu}{2E_h} L^{\mu\nu} w^{N\,s.i.}_{\mu\nu}(\tilde{p}_N,P_h,\lambda'\lambda) \quad (19)$$

represents the corresponding cross section for the scattering of a charged lepton from a polarized moving nucleon. In Eq. (18), $\tilde{\alpha}$ is given by

$$\tilde{\alpha} \equiv \frac{(p_N\cdot k)}{\mathcal{E} m_N} \quad (20)$$

and is usually called the "flux factor." When energies are close to the Bjorken limit, $\tilde{\alpha}$ coincides with the light-cone momentum fraction of the nucleon inside the nucleus, i.e.,

$$\lim_{\to Bj}\tilde{\alpha} = \frac{A(p_N\cdot q)}{(P_A\cdot q)}\,. \quad (21)$$

## III. THE DISTORTED SPIN-DEPENDENT SPECTRAL FUNCTION

In order to go beyond PWIA [cf. Eq. (4)], it is necessary to deal with the FSI between the debris, originating from the struck nucleon, and the fully interacting $(A-1)$ nuclear system. In view of this, the dependence upon the space coordinates in the current operator is kept, since we will focus on the action of the current onto the final state in coordinate space.

The starting point is the hadronic tensor written as follows:

$$W^{s.i.}_{\mu\nu}(\mathbf{S}_A,Q^2,P_h) = \frac{1}{2M_A}\sum_X \langle\, S_A,P_A|\hat{J}_\mu(\hat{\mathbf{r}}_i)|P_h,X\,\rangle \times \langle\, P_h,X|\hat{J}_\nu(\hat{\mathbf{r}}_i)|S_A,P_A\,\rangle \times \delta(M_A+\nu-E_X-E_h)d\tau_X. \quad (22)$$

For a $^3$He target, the matrix element of the current operator $\hat{J}_\mu(\hat{\mathbf{r}}_1,\hat{\mathbf{r}}_2,\hat{\mathbf{r}}_3)$ between the nuclear ground state, $|\Psi^{\mathbf{S}_A}_3(1,2,3)\,\rangle$, and a generic final state, $|\Psi^f(1,2,3)\,\rangle$, is evaluated by introducing the following approximation:

$$\hat{J}_\mu(\hat{\mathbf{r}}_1,\hat{\mathbf{r}}_2,\hat{\mathbf{r}}_3) \approx \sum_i \hat{j}_\mu(\mathbf{r}_i), \quad (23)$$

where $\hat{j}_\mu(\mathbf{r}_i)$ is the one-body transition current operator that describes the electromagnetic response of the single nucleon inside the target. In this way, the matrix element becomes

$$\begin{aligned}&\langle\, P_h,X|\hat{J}_\mu(\hat{\mathbf{r}}_1,\hat{\mathbf{r}}_2,\hat{\mathbf{r}}_3)|\mathbf{S}_3,P_3\,\rangle \\ &= \langle\,\Psi^f(1,2,3)|\hat{J}_\mu(\hat{\mathbf{r}}_1,\hat{\mathbf{r}}_2,\hat{\mathbf{r}}_3)|\Psi^{\mathbf{S}_3}_3(1,2,3)\,\rangle \\ &\approx \sum_i\langle\,\Psi^f(1,2,3)|\hat{j}_\mu(\hat{\mathbf{r}}_i)|\Psi^{\mathbf{S}_3}_3(1,2,3)\,\rangle \\ &= 3\langle\,\Psi^f(1,2,3)|\hat{j}_\mu(\hat{\mathbf{r}}_1)|\Psi^{\mathbf{S}_3}_3(1,2,3)\,\rangle. \end{aligned} \quad (24)$$

In what follows, for the sake of concreteness, the active nucleon is labeled $i=1$ and the spectator indexes are 23.

For constructing a realistic approximation of FSI, it is useful to consider that, in the SIDIS processes we aim to investigate, the momentum transfer $\mathbf{q}$ is rather large, and therefore $h$, the leading pseudoscalar meson to be detected, and $X'$, which has baryon number equal to 1 [cf. Eq. (4)], move throughout the $A-1$ remnants with high velocity. This observation motivates the introduction of the generalized eikonal approximation (see, e.g., Refs. [33,38] and references quoted therein) for estimating the rest of FSI not taken into account through PWIA

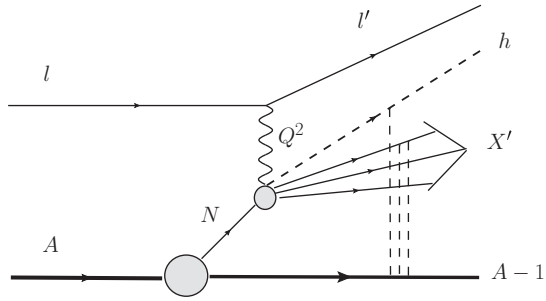


FIG. 1. The SIDIS process $A(e,e'h)X$, with final state interactions taken into account.

[cf. Eq. (4)]. Then, the final state can be approximated in coordinate space as

$$\langle \mathbf{r}_1\mathbf{r}_2\mathbf{r}_3|\Psi^f(1,2,3)\rangle \approx \frac{\mathcal{A}}{\sqrt{V}\sqrt{3}}\Psi^f_{23}(\mathbf{r}_2,\mathbf{r}_3)\chi_{\lambda_Y}\phi(\xi_Y) \times \sqrt{2E_Y}e^{i\mathbf{p}_Y\cdot\mathbf{r}_1}\mathcal{G}(\mathbf{r}_1,\mathbf{r}_2,\mathbf{r}_3), \quad (25)$$

where $\mathcal{A}$ is the antisymmetrization operator that acts on the final state, given by a recoiling two-nucleon system and a debris $Y$ originated by the struck nucleon (see below), $\Psi^f_{23}(\mathbf{r}_2,\mathbf{r}_3)$ is the properly antisymmetrized wave function of the recoiling two-nucleon system, $V$ is the normalization volume of the global motion of the final state, and the amplitude $\mathcal{G}(\mathbf{r}_1,\mathbf{r}_2,\mathbf{r}_3)$, identically equal to 1 in PWIA, is the nonsingular part of the matrix elements of the Glauber operator, i.e.,

$$\langle \mathbf{r}'_1,\mathbf{r}'_2,\mathbf{r}'_3|\hat{\mathcal{G}}|\mathbf{r}_1,\mathbf{r}_2,\mathbf{r}_3\rangle = \delta(\mathbf{r}'_1-\mathbf{r}_1)\delta(\mathbf{r}'_2-\mathbf{r}_2) \times \delta(\mathbf{r}'_3-\mathbf{r}_3)\mathcal{G}(\mathbf{r}_1,\mathbf{r}_2,\mathbf{r}_3). \quad (26)$$

The Glauber amplitude depends only upon intrinsic coordinates, $\mathbf{r},\boldsymbol{\rho}$, related to $\mathbf{r}_i$ through

$$\mathbf{r}_1 = \tfrac{2}{3}\boldsymbol{\rho}+\mathbf{R}, \quad \mathbf{r}_2 = -\tfrac{1}{3}\boldsymbol{\rho}+\tfrac{1}{2}\mathbf{r}+\mathbf{R}, \quad \mathbf{r}_3 = -\tfrac{1}{3}\boldsymbol{\rho}-\tfrac{1}{2}\mathbf{r}+\mathbf{R}, \quad (27)$$

and therefore

$$\mathcal{G}(\mathbf{r}_1,\mathbf{r}_2,\mathbf{r}_3) \to \mathcal{G}(\mathbf{r},\boldsymbol{\rho}). \quad (28)$$

In Eq. (25), $Y$ is the final debris produced by the nucleon after the absorption of the virtual photon. In the process under consideration, it coincides with a leading pseudoscalar meson to be detected and a baryonic remnant $X'$ (cf. Fig. 1). The function $\phi(\xi_Y)$ characterizes the internal structure of the debris that will hadronize in $h+X'$, $\chi_{\lambda_Y}$ is its spin state, while $e^{i\mathbf{p}_Y\mathbf{r}_1}$ is the plane wave describing the propagation of the c.m. of the debris.

By using intrinsic coordinates, the final state in Eq. (25) becomes

$$\langle \mathbf{r}_1\mathbf{r}_2\mathbf{r}_3|\Psi^f(1,2,3)\rangle \approx \frac{\mathcal{A}}{\sqrt{V}\sqrt{3}}\sqrt{2E_Y}e^{i\mathbf{p}_Y\cdot(2\boldsymbol{\rho}/3+\mathbf{R})}\chi_{\lambda_Y}\phi(\xi_Y) \times \sqrt{2E_{23}}e^{i\mathbf{P}_{23}\cdot(\mathbf{R}-\boldsymbol{\rho}/3)}\phi^{f_{23}}_{\epsilon^*_{23}}(\mathbf{r})\mathcal{G}(\mathbf{r},\boldsymbol{\rho}), \quad (29)$$

where $\mathbf{P}_{23}$ is the total momentum of the (2,3) system and the intrinsic part of the two-nucleon state, $\phi^{f_{23}}_{\epsilon^*_{23}}(\mathbf{r})$, has quantum numbers $f_{23}$ and energy eigenvalue $\epsilon^*_{23}$.

Disregarding the photon coupling to the spectator pair, one can apply the familiar approximation

$$\langle \Psi^f(1,2,3)|\hat{j}_\mu(\hat{\mathbf{r}}_1)|\Psi^{\mathbf{S}_3}_3(1,2,3)\rangle \approx \frac{1}{\sqrt{3}\sqrt{V}}\sqrt{2E_Y}\int d\mathbf{r}_1 d\mathbf{r}_2 d\mathbf{r}_3 \Psi^{*f}_{23}(\mathbf{r}_2,\mathbf{r}_3)e^{-i\mathbf{p}_Y\cdot\mathbf{r}_1}\chi^+_{\lambda_Y} \times \phi^*(\xi_Y)\mathcal{G}(\mathbf{r}_1,\mathbf{r}_2,\mathbf{r}_3)\hat{j}_\mu(\mathbf{r}_1)\Psi^{\mathbf{S}_3}_3(\mathbf{r}_1,\mathbf{r}_2,\mathbf{r}_3), \quad (30)$$

with

$$\Psi^{\mathbf{S}_3}_3(\mathbf{r}_1,\mathbf{r}_2,\mathbf{r}_3) = \sqrt{2E_3}e^{i\mathbf{P}_3\cdot\mathbf{R}}\psi^{\mathbf{S}_3}_3(\mathbf{r},\rho) = \sqrt{2M_3}\psi^{\mathbf{S}_3}_3(\mathbf{r},\rho), \quad (31)$$

where $\psi^{\mathbf{S}_3}_3(\mathbf{r},\rho)$ is the intrinsic nuclear wave function and the total momentum of the nucleus is $\mathbf{P}_3=0$.

Moreover, if $\mathcal{G}(\mathbf{r}_1,\mathbf{r}_2,\mathbf{r}_3)$ is such that (i) it does not depend upon spins and (ii) it commutes with $\hat{j}_\mu(\mathbf{r}_1)$ (as it does in PWIA, since $\mathcal{G}(\mathbf{r}_1,\mathbf{r}_2,\mathbf{r}_3)\equiv 1$), one can write

$$\langle \Psi^f(1,2,3)|\hat{j}_\mu(\hat{\mathbf{r}}_1)|\Psi^{\mathbf{S}_3}_3(1,2,3)\rangle \approx \frac{1}{\sqrt{3}\sqrt{V}}\sqrt{2E_Y}\int d\mathbf{r}_1 d\mathbf{r}_2 d\mathbf{r}_3 \Psi^{*f}_{23}(\mathbf{r}_2,\mathbf{r}_3)e^{-i\mathbf{p}_Y\cdot\mathbf{r}_1}\chi^+_{\lambda_Y} \times \phi^*(\xi_Y)\hat{j}_\mu(\mathbf{r}_1)\mathcal{G}(\mathbf{r}_1,\mathbf{r}_2,\mathbf{r}_3)\Psi^{\mathbf{S}_3}_3(\mathbf{r}_1,\mathbf{r}_2,\mathbf{r}_3). \quad (32)$$

This is the main assumption of our approach, that is exact when the one-body operator $\hat{j}_\mu$ does not contain the momentum $\hat{\mathbf{p}}$. Otherwise, one can have a nonzero commutator $[\hat{j}_\mu,\mathcal{G}]$. In the present SIDIS case, the explicit expression of the transition current operator $\hat{j}_\mu$ is unknown and we cannot compute the commutator, but we assume a vanishing result, namely $[\hat{\mathbf{p}},\mathcal{G}(1,2,3)] \sim \partial/\partial\boldsymbol{\rho}\,\mathcal{G}(\mathbf{r},\boldsymbol{\rho}) \sim 0$. It is worth noting that if only the longitudinal part of the current operator is relevant and the dependence on the coordinates in the Glauber operator is mainly given by the transverse components, one can largely justify our assumption. As a matter of fact, we adopt in the following the same approach used in Ref. [38], where the distorted spectral function was evaluated only in the 2bbu channel. This amounts to consider GEA (see, e.g., Ref. [33] and references therein). In this scheme, the Glauber amplitude reads

$$\mathcal{G}(\mathbf{r}_1,\mathbf{r}_2,\mathbf{r}_3) = \prod_{i=2,3}[1-\theta(\mathbf{r}_{i||}-\mathbf{r}_{1||})\Gamma \times (\mathbf{r}_{i\perp}-\mathbf{r}_{1\perp},\mathbf{r}_{i||}-\mathbf{r}_{1||})], \quad (33)$$

where the parallel and perpendicular components of the vectors $\mathbf{r}_i$ are determined with respect to $\mathbf{p}_Y$, i.e., to the direction of propagation of the debris. In DIS, when $|\mathbf{q}|^2 \gg |\mathbf{p}_N|^2$, this direction coincides with the direction of $\mathbf{q}$. The profile function $\Gamma(\mathbf{r}_{i\perp}-\mathbf{r}_{1\perp},\mathbf{r}_{i||}-\mathbf{r}_{1||})$ in Eq. (33), unlike in the standard Glauber approach, depends not only upon the transverse relative separation but also upon the longitudinal one. The Heaviside function $\theta(\mathbf{r}_{i||}-\mathbf{r}_{1||})$ assures causality in the rescattering process. In the following, we adopt for $\Gamma(\mathbf{r}_{i\perp}-\mathbf{r}_{1\perp},\mathbf{r}_{i||}-\mathbf{r}_{1||})$ the expression already used in Refs. [33,38], based on the

hadronization model of Ref. [35] to evaluate the total cross section of the debris-nucleon interaction, depending on the kinematics of the process, viz.,

$$\Gamma(\mathbf{r}_{i\perp}-\mathbf{r}_{1\perp},\mathbf{r}_{i||}-\mathbf{r}_{1||}) = \frac{(1-i\eta)\sigma_{\rm eff}(\mathbf{r}_{i||}-\mathbf{r}_{1||})}{4\pi b_0}\exp\left[-\frac{(\mathbf{r}_{i\perp}-\mathbf{r}_{1\perp})^2}{2b_0^2}\right]. \quad (34)$$

In this approach, the resulting Glauber operator turns out to be mildly dependent on the longitudinal distance, so that the assumption of a vanishing commutator between the operator and the current is qualitatively justified in the present scheme. Details on the model and on the corresponding parameters can be found in Refs. [33,38].

An important issue has now to be addressed. The effective cross section, $\sigma_{\rm eff}$, in Eq. (32), models the hadronization of the debris interacting with the recoiling nuclear system. The debris consists of one nucleon and radiated mesons and gluons. The number of radiated gluons depends on the momentum scale of the process, given by $Q^2$. Besides the emission of mesons and gluons will stop when a maximum longitudinal distance is reached, which increases with the invariant mass, $W_Y$, of the debris. As a consequence, $\sigma_{\rm eff}$ depends also on $W_Y$. Therefore, in Eq. (34), one should write $\sigma_{\rm eff}(\mathbf{r}_{i||}-\mathbf{r}_{1||},Q^2,W_Y)$ and not simply $\sigma_{\rm eff}(\mathbf{r}_{i||}-\mathbf{r}_{1||})$. Nevertheless, in the kinematics we are going to discuss in this paper it occurs that (i) for a given value of $\mathcal{E}$, the range of variation of $Q^2$ is not wide enough to produce important changes in the gluon radiation rate and (ii) $\sigma_{\rm eff}$ depends weakly on the maximum longitudinal distance. In other words, in the kinematics we are going to analyze, for a given $\mathcal{E}$, the dependence of $\sigma_{\rm eff}$ on $Q^2$ and $W_Y$ is weak. As a matter of fact, in Refs. [33,38], $\sigma_{\rm eff}(\mathbf{r}_{i||}-\mathbf{r}_{1||},Q^2,W_Y)\simeq\sigma_{\rm eff}(\mathbf{r}_{i||}-\mathbf{r}_{1||})$ was assumed in actual calculations. In Ref. [33], the model of $\sigma_{\rm eff}$ with this assumption was proven to be able to reasonably describe data of Ref. [44] for unpolarized spectator SIDIS processes, in a kinematics which is close to the one we are discussing. Therefore, to avoid a too heavy notation, throughout the paper we drop the dependence of $\sigma_{\rm eff}$ on $Q^2$ and $W_Y$ in the relevant expressions.

For completeness we mention that, in the actual form for $\mathcal{G}(\mathbf{r},\boldsymbol{\rho})$, Eq. (33), there is a $\theta$ function that generates a contribution to the commutator proportional to $\delta^3(\boldsymbol{\rho})$. Obviously, such a contribution is vanishing if not too severe singularities are present in both target and spectator wave functions. It is worth noticing that in the quasielastic case, where an explicit form of the current operator is commonly accepted, the above assumption, called the *factorized form* of FSI, has been discussed against the unfactorized one in Ref. [45].

Coming back to Eq. (32) and following the spirit of the standard procedure adopted in PWIA, one can insert the one-nucleon completeness [cf. Eq. (5)]

$$\sum_\lambda\int\frac{d\mathbf{k}}{2E_k(2\pi)^3}|k,\lambda\rangle\langle k,\lambda| = I, \quad (35)$$

where $I$ is the identity, and the free nucleon states $|k,\lambda\rangle$ are normalized according to $\langle k,\lambda|k',\lambda'\rangle = 2E_k\delta_{\lambda\lambda'}(2\pi)^3\delta(\mathbf{k}-\mathbf{k}')$. Then, one can obtain from Eq. (32) the following expression:

$$\langle\Psi^f(1,2,3)|\hat{j}_\mu(\hat{\mathbf{r}}_1)|\Psi_3^{\mathbf{S}_3}(1,2,3)\rangle \approx \frac{1}{\sqrt{3}\sqrt{V}}\int\frac{d\mathbf{k}}{(2\pi)^3 2E_k}\sum_\lambda\langle p_Y,\lambda_Y;\phi(\xi_Y)|\hat{j}_\mu(\hat{\mathbf{r}}_1')|k,\lambda\rangle\left[\sqrt{2E_k}\int d\mathbf{r}_1 d\mathbf{r}_2 d\mathbf{r}_3\,\chi_\lambda^\dagger e^{-i\mathbf{k}\cdot\mathbf{r}_1}\Psi_{23}^{*f}(\mathbf{r}_2,\mathbf{r}_3)\,\mathcal{G}(\mathbf{r}_1,\mathbf{r}_2,\mathbf{r}_3)\Psi_3^{\mathbf{S}_3}(\mathbf{r}_1,\mathbf{r}_2,\mathbf{r}_3)\right]. \quad (36)$$

By changing coordinates [see Eq. (29)] and exploiting the translation invariance of the initial vertex in Eq. (10), one gets for Eq. (36)

$$\begin{aligned}\langle\Psi^f(1,2,3)|\hat{j}_\mu(\hat{\mathbf{r}}_1)|\Psi_3^{\mathbf{S}_3}(1,2,3)\rangle &\approx \frac{1}{\sqrt{3}\sqrt{V}}\sum_\lambda\int\frac{d\mathbf{k}}{(2\pi)^3 2E_k}\langle p_Y,\lambda_Y\phi(\xi_Y)|\hat{j}_\mu(0)|k,\lambda\rangle(2\pi)^3\delta(\mathbf{q}+\mathbf{k}-\mathbf{p}_Y)(2\pi)^3\sqrt{2E_k 2E_{23}2M_3}\delta(\mathbf{k}+\mathbf{P}_{23})\\ &\times\int d\mathbf{r}d\boldsymbol{\rho}\left[\chi_\lambda^\dagger e^{-i2\mathbf{k}\cdot\boldsymbol{\rho}/3}e^{i\mathbf{P}_{23}\cdot\boldsymbol{\rho}/3}\phi_{\epsilon_{23}^*}^{f_{23}*}(\mathbf{r})\mathcal{G}(\mathbf{r},\boldsymbol{\rho})\Psi_3^{\mathbf{S}_3}(\mathbf{r},\boldsymbol{\rho})\right]\\ &= \frac{(2\pi)^3}{\sqrt{3}\sqrt{2E_{\rm mis}V}}\sqrt{2E_{23}2M_3}\delta(\mathbf{q}-\mathbf{p}_{\rm mis}-\mathbf{p}_Y)\sum_\lambda\langle p_Y,\lambda_Y\phi(\xi_Y)|\hat{j}_\mu(0)|p_{\rm mis},\lambda\rangle\int d\mathbf{r}d\boldsymbol{\rho}\left[\chi_\lambda^\dagger e^{i\mathbf{p}_{\rm mis}\cdot\boldsymbol{\rho}}\phi_{\epsilon_{23}^*}^{f_{23}*}(\mathbf{r})\mathcal{G}(\mathbf{r},\boldsymbol{\rho})\Psi_3^{\mathbf{S}_3}(\mathbf{r},\boldsymbol{\rho})\right],\end{aligned} \quad (37)$$

where $\langle p_Y,\lambda_Y\phi(\xi_Y)|\hat{j}_\mu(0)|k,\lambda\rangle$ is the matrix element of the unknown transition current operator involved in the quark-photon vertex (notice that the factor $\sqrt{2E_Y 2E_k}$ is put inside the matrix element), and $p_{\rm mis}\equiv\{E_{\rm mis}=\sqrt{M_N^2+|\mathbf{p}_{\rm mis}|^2},-\mathbf{p}_{\rm mis}\}$, with $\mathbf{p}_{\rm mis}=\mathbf{q}-\mathbf{p}_Y=\mathbf{P}_{23}$ being the three-momentum of the system "23" in the final state, $\Psi_{23}^f(\mathbf{r}_2,\mathbf{r}_3)$. Indeed, $\mathbf{p}_{\rm mis}$ is also the three-momentum of the initial spectator system and eventually of the nucleon (with opposite sign) before absorbing the virtual photon. This is a consequence of the assumed commutativity between the one-body current and the Glauber amplitude. It should be pointed out that the matrix element $\langle p_Y,\lambda_Y\phi(\xi_Y)|\hat{j}_\mu(0)|p_{\rm mis}\lambda\rangle$ describes SIDIS off a free nucleon, within our approach.

Summarizing the above results and recalling that $X \to (A-1)\otimes Y \to (A-1)\otimes h \otimes X'$, one can write the hadron tensor for a polarized $^3$He target as follows:

$$
\begin{aligned}
W^{s.i.}_{\mu\nu}(\mathbf{S_3},Q^2,P_h) &= \frac{1}{2M_3}\sum_X \langle\, S_3,P_3|\hat{J}_\mu|P_h,X\,\rangle\langle\, P_h,X|\hat{J}_\nu|S_3,P_3\,\rangle\delta(M_3+\nu-E_{X'}-E_h-E_{23})d\tau_X \\
&\approx \frac{3}{V}(2\pi)^3\sum_{X'}d\tau'_X\sum_{f_{23}}\sum\!\!\!\!\!\!\int_{\epsilon^*_{23}}\rho(\epsilon^*_{23})\int\frac{d\mathbf{p}_{\rm mis}}{2E_{\rm mis}}\delta(M_3+\nu-E_{X'}-E_h-E_{23}) \\
&\quad\times\delta(\mathbf{q}-\mathbf{p}_{\rm mis}-\mathbf{p}_h-\mathbf{p}_{X'})\sum_\lambda\langle\, p_Y,\lambda_Y\phi(\xi_Y)|\hat{j}_\mu(0)|p_{\rm mis},\lambda\,\rangle\int d\mathbf{r}d\boldsymbol{\rho}\big[\chi^\dagger_\lambda e^{i\mathbf{p}_{\rm mis}\cdot\boldsymbol{\rho}}\phi^{f_{23}*}_{\epsilon^*_{23}}(\mathbf{r})\mathcal{G}(\mathbf{r},\boldsymbol{\rho})\Psi^{\mathbf{S}_3}_3(\mathbf{r},\boldsymbol{\rho})\big] \\
&\quad\times\delta(\mathbf{q}-\mathbf{p}_{\rm mis}-\mathbf{p}_h-\mathbf{p}_{X'})\sum_{\lambda'}\langle\, p_{\rm mis},\lambda'|\hat{j}_\mu(0)|\phi(\xi_Y)p_Y,\lambda_Y\,\rangle\int d\mathbf{r}d\boldsymbol{\rho}\big[\chi^\dagger_{\lambda'}e^{i\mathbf{p}_{\rm mis}\cdot\boldsymbol{\rho}}\phi^{f_{23}*}_{\epsilon^*_{23}}(\mathbf{r})\mathcal{G}(\mathbf{r},\boldsymbol{\rho})\Psi^{\mathbf{S}_3}_3(\mathbf{r},\boldsymbol{\rho})\big]^* \\
&= 3(2\pi)^3\sum_{X'}d\tau'_X\sum_{f_{23}}\sum\!\!\!\!\!\!\int_{\epsilon^*_{23}}\rho(\epsilon^*_{23})\int\frac{d\mathbf{p}_{\rm mis}}{2E_{\rm mis}}\delta(M_3+\nu-E_{X'}-E_h-E_{23})\delta(\mathbf{q}-\mathbf{p}_{\rm mis}-\mathbf{p}_h-\mathbf{p}_{X'}) \\
&\quad\times\sum_\lambda\langle\, p_Y,\lambda_Y\phi(\xi_Y)|\hat{j}_\mu(0)|p_{\rm mis},\lambda\,\rangle\int d\mathbf{r}d\boldsymbol{\rho}\big[\chi^\dagger_\lambda e^{i\mathbf{p}_{\rm mis}\cdot\boldsymbol{\rho}}\phi^{f_{23}*}_{\epsilon^*_{23}}(\mathbf{r})\mathcal{G}(\mathbf{r},\boldsymbol{\rho})\Psi^{\mathbf{S}_3}_3(\mathbf{r},\boldsymbol{\rho})\big] \\
&\quad\times\sum_{\lambda'}\langle\,\lambda',p_{\rm mis}|\hat{j}_\mu(0)|\phi(\xi_Y)p_Y,\lambda_Y\,\rangle\int d\mathbf{r}d\boldsymbol{\rho}\big[\chi^\dagger_{\lambda'}e^{i\mathbf{p}_{\rm mis}\cdot\boldsymbol{\rho}}\phi^{f_{23}*}_{\epsilon^*_{23}}(\mathbf{r})\mathcal{G}(\mathbf{r},\boldsymbol{\rho})\Psi^{\mathbf{S}_3}_3(\mathbf{r},\boldsymbol{\rho})\big]^*, \qquad (38)
\end{aligned}
$$

where $\mathbf{p}_Y=\mathbf{p}_h+\mathbf{X}'$ has been inserted and the following phase space of the spectator system has been adopted:

$$
\sum_{f_{23}}\sum\!\!\!\!\!\!\int_{\epsilon^*_{23}}\rho(\epsilon^*_{23})\int\frac{d\mathbf{P}_{23}}{(2\pi)^3 2E_{23}}=\sum_{f_{23}}\sum\!\!\!\!\!\!\int_{\epsilon^*_{23}}\rho(\epsilon^*_{23})\int\frac{d\mathbf{p}_{\rm mis}}{(2\pi)^3 2E_{23}}. \qquad (39)
$$

In conclusion, the nuclear hadronic tensor reads

$$
W^{s.i.}_{\mu\nu}(\mathbf{S_3},Q^2,P_h)=\sum_{\lambda\lambda'}\sum_N\int d\mathbf{p}_{\rm mis}\int dE\,\frac{m_N}{E_{\rm mis}}w^{N\,s.i.}_{\mu\nu}(\tilde{p}_{\rm mis},P_h,\lambda'\lambda)\mathcal{P}^{N\,\mathbf{S}_3}_{\lambda\lambda'}(E,\mathbf{p}_{\rm mis}), \qquad (40)
$$

where the semi-inclusive nucleon tensor [cf. Eq. (17)] is given by

$$
w^{N\,s.i.}_{\mu\nu}(-\tilde{p}_{\rm mis},P_h,\lambda'\lambda)=\frac{1}{2m_N}\sum_{X'}\langle\, p_{\rm mis},\lambda'|\hat{j}^N_\mu|P_h,X'\,\rangle\langle\, P_h,X'|\hat{j}^N_\nu|p_{\rm mis},\lambda\,\rangle\delta^4(q-\tilde{p}_{\rm mis}-P_h-P_{X'})d\tau_{X'}\,, \qquad (41)
$$

with $\tilde{p}_{\rm mis}\equiv\{E-m_N,\mathbf{p}_{\rm mis}\}$ and the isospin formalism has been released (i.e., $3\to\sum_N$). Equation (40) introduced the *distorted* spin-dependent spectral function given by the following expression for a polarized $^3$He target,

$$
\mathcal{P}^{N\,\mathbf{S}_3}_{\lambda\lambda'}(E,\mathbf{p}_{\rm mis})=\sum_{f_{23}}\sum\!\!\!\!\!\!\int_{\epsilon^*_{23}}\rho(\epsilon^*_{23})\,\tilde{\mathcal{O}}^{N\,\mathbf{S}_3\,f_{23}}_{\lambda\lambda'}(\epsilon^*_{23},\mathbf{p}_{\rm mis})\,\delta(E+M_3-m_N-M^*_{23}), \qquad (42)
$$

with the product of distorted overlaps defined by

$$
\tilde{\mathcal{O}}^{N\,\mathbf{S}_3\,f_{23}}_{\lambda\lambda'}(\epsilon^*_{23},\mathbf{p}_{\rm mis})=\big\langle\,\lambda,e^{-i\mathbf{p}_{\rm mis}\cdot\boldsymbol{\rho}}\phi^{f_{23}}_{\epsilon^*_{23}}(\mathbf{r})\mathcal{G}(\mathbf{r},\boldsymbol{\rho})\big|\Psi^{\mathbf{S}_3}_3(\mathbf{r},\boldsymbol{\rho})\big\rangle\big\langle\,\Psi^{\mathbf{S}_3}_3(\mathbf{r}',\boldsymbol{\rho}')\big|\mathcal{G}(\mathbf{r}',\boldsymbol{\rho}')\phi^{f_{23}}_{\epsilon^*_{23}}(\mathbf{r}')e^{-i\mathbf{p}_{\rm mis}\cdot\boldsymbol{\rho}'},\lambda'\big\rangle, \qquad (43)
$$

with an obvious meaning of the adopted notation (see Appendix A for the detailed expression of the overlaps).

One should notice that the distorted spectral function depends, through the profile function Eq. (34), on the effective cross section $\sigma_{\rm eff}(\mathbf{r}_{i||}-\mathbf{r}_{1||})$. As discussed above, below Eq. (34), this quantity depends, in principle, also on $Q^2$ and $W_Y$. As a consequence, the distorted spectral function is a process-dependent quantity, at variance with the spectral function evaluated in PWIA. In principle, at any kinematical point (given by $\mathcal{E},\theta_e,x_{Bj}$, and $\theta_{p_{\rm mis}q}$), one should evaluate a different distorted spectral function. Nevertheless, for the reasons discussed below Eq. (32), in the kinematics we are going to study, for a fixed initial electron energy $\mathcal{E}$ and scattering angle $\theta_e$, the dependence of $\sigma_{\rm eff}$ on $Q^2$ and $W_Y$ is rather mild and can be disregarded. As a consequence, also the spectral function, for fixed $\mathcal{E}$ and $\theta_e$, can be considered independent on $x_{Bj}$ and $\theta_{p_{\rm mis}q}$. To avoid heavy notation, this dependence is not shown throughout the paper.

The generalization of the above formalism to a polarized nuclear target with $A$ nucleon is straightforward. In particular, for the nuclear cross section $\sigma^A(\mathbf{S}_A) \equiv \frac{d\sigma(\mathbf{S}_A)}{d\varphi_e dx_{Bj} dy d\mathbf{P}_h}$, one has

$$\sigma^A(\mathbf{S}_A) = \sum_{\lambda\lambda'} \sum_N \int d\mathbf{p}_{\rm mis} \int dE \frac{\tilde{\alpha} m_N}{E_N} \sigma^N_{\lambda\lambda'} \mathcal{P}^{N\,\mathbf{S}_A}_{\lambda\lambda'}(E, \mathbf{p}_{\rm mis}). \tag{44}$$

One should notice that, formally, Eq. (40) coincides with Eq. (16), relative to the PWIA case, if the distorted spectral function is substituted by the PWIA one. This is a consequence of the assumption made between Eqs. (30) and (32), concerning the commutation property of the Glauber operator with the nucleon current. The FSI described in this manner, called factorized FSI in the literature (see, e.g., Ref. [45] and references therein), lead to convolution-like formulas, as the ones obtained in the PWIA case, where the distorted spectral function appears instead of the PWIA one. The latter can be recovered just putting the Glauber operator identically equal to 1. This observation has crucial consequences in the following sections of the present paper.

It is clear that our model for the FSI could benefit from a comparison of our theoretical results against absolute cross section of SIDIS processes off a polarized $^3$He target. Unfortunately, no paper dealing with SIDIS cross sections off a polarized $^3$He is available. Eventually, very recently, a paper has been published by the Hall A Collaboration at JLab, which concerns the unpolarized sector only [46].

Since it is important to check our reaction model, within PWIA or including FSI, we plan to accurately and widely analyze these new data possibly in strict contact with experimental collaborations to plan future investigations of the SIDIS cross sections.

## IV. THE DEPENDENCE OF THE NUCLEAR HADRONIC TENSOR UPON THE TARGET NUCLEUS POLARIZATION

As a matter of fact, the whole formalism developed in the PWIA case in Ref. [31] can be exploited now in the present scenario, once the distorted overlaps are properly evaluated and inserted in the relevant equations.

Notice that, in PWIA, the spectral function $P^{\mathbf{S}_3}_{\lambda\lambda}(E, \mathbf{p}_{\rm mis})$ in (42) defines the probability distribution to remove from a polarized $^3$He with polarization $\mathbf{S}_3$ a polarized nucleon with momentum $-\mathbf{p}_{\rm mis}$ and polarization $\mathbf{s}_N$ (characterized by spin projection $\lambda$ on the quantization axis) leaving the remnant $(A-1)$ system with removal energy $E$. Once the full FSI is taken into account, even through GEA, the probabilistic interpretation of the distorted spectral function is somehow lost.

A further issue is represented by the fact that the direction of the target polarization axis, $\mathbf{S}_3$, may not always be parallel to the direction which determines the eikonal $\mathcal{G}$ matrix, i.e., the direction of $\mathbf{p}_Y$ (or, in DIS, the direction of $\mathbf{q}$). In particular, in the SIDIS process of interest here, the target nucleus is transversely polarized, i.e., $\mathbf{S}_3 \perp \mathbf{q}$. To reconcile the polarization axis and the eikonal approximation, one needs to rotate the quantization axis of the target wave function from the direction of $\mathbf{q}$ to the direction of the polarization $\mathbf{S}_3$, namely

$$\begin{aligned} &\langle \theta,\phi|\Psi_{^3\rm He}\rangle_{\hat{\mathbf{S}}_3} \\ &= \langle \theta',\phi'|D^{1/2}(0,\beta,0)|\Psi_{^3\rm He}\rangle_{\hat{\mathbf{q}}} = \cos(\beta/2) \\ &\quad \times \left\langle \theta',\phi' \middle| \Psi^{M=1/2}_{^3\rm He} \right\rangle_{\hat{\mathbf{q}}} + \sin(\beta/2) \left\langle \theta',\phi' \middle| \Psi^{M=-1/2}_{^3\rm He} \right\rangle_{\hat{\mathbf{q}}}, \end{aligned} \tag{45}$$

where the subscript indicates the direction of the quantization axis, $\cos\beta = \hat{\mathbf{S}}_3 \cdot \hat{\mathbf{q}}$, and the polarization vector $\mathbf{S}_3$ is supposed to be in the $(x,z)$ plane. In Eq. (45), $D^{1/2}_{\sigma'\sigma}$ are the suitable Wigner $D$ functions [47]. Therefore in the general case, the nuclear tensor in Eq. (40) is modified and reads

$$\begin{aligned} W^{s.i.}_{\mu\nu}(\mathbf{S}_3, Q^2, P_h) &= \cos^2(\beta/2)\, W^{\frac{1}{2}\frac{1}{2}}_{\mu\nu} + \sin^2(\beta/2) W^{-\frac{1}{2}-\frac{1}{2}}_{\mu\nu} \\ &\quad + \sin\beta \left[\tfrac{1}{2}\left(W^{\frac{1}{2}-\frac{1}{2}}_{\mu\nu} + W^{-\frac{1}{2}\frac{1}{2}}_{\mu\nu}\right)\right], \end{aligned} \tag{46}$$

$$\begin{aligned} W^{s.i.}_{\mu\nu}(-\mathbf{S}_3, Q^2, P_h) &= \sin^2(\beta/2)\, W^{\frac{1}{2}\frac{1}{2}}_{\mu\nu} + \cos^2(\beta/2) W^{-\frac{1}{2}-\frac{1}{2}}_{\mu\nu} \\ &\quad - \sin\beta \left[\tfrac{1}{2}\left(W^{\frac{1}{2}-\frac{1}{2}}_{\mu\nu} + W^{-\frac{1}{2}\frac{1}{2}}_{\mu\nu}\right)\right]. \end{aligned} \tag{47}$$

In the above equations, we have defined

$$\begin{aligned} W^{MM'}_{\mu\nu} &= \sum_{\lambda\lambda'} \sum_N \int d\mathbf{p}_{\rm mis} \int dE \frac{m_N}{E_N} w^{N\,s.i.}_{\mu\nu}(-\tilde{p}_{\rm mis}, P_h, \lambda'\lambda) \\ &\quad \times \mathcal{P}^{N\,MM'}_{\lambda\lambda'}(E, \mathbf{p}_{\rm mis}), \end{aligned} \tag{48}$$

where the third components $M$ and $M'$ are defined with respect to the direction $\hat{\mathbf{q}}$. In Eq. (48) one has [cf. Eq. (42)]

$$\begin{aligned} \mathcal{P}^{N\,MM'}_{\lambda\lambda'}(E, \mathbf{p}_{\rm mis}) &= \sum_{f_{23}} \sum\!\!\!\!\!\!\int_{\epsilon^*_{23}} \rho(\epsilon^*_{23})\, \tilde{\mathcal{O}}^{N\,MM'\,f_{23}}_{\lambda\lambda'}(\epsilon^*_{23}, \mathbf{p}_{\rm mis}) \\ &\quad \times \delta(E + M_3 - m_N - M^*_{23}), \end{aligned} \tag{49}$$

with $\tilde{\mathcal{O}}^{N\,M\,M'\,f_{23}}_{\lambda\lambda'}$, a natural nondiagonal generalization of Eq. (43), viz.,

$$\begin{aligned} &\tilde{\mathcal{O}}^{N\,M\,M'\,f_{23}}_{\lambda\lambda'}(\epsilon^*_{23}, \mathbf{p}_{\rm mis}) \\ &\quad = \left\langle \lambda, e^{-i\mathbf{p}_{\rm mis}\cdot\boldsymbol{\rho}} \phi^{f_{23}}_{\epsilon^*_{23}}(\mathbf{r}) \mathcal{G}(\mathbf{r},\boldsymbol{\rho}) |\Psi^M_3(\mathbf{r},\boldsymbol{\rho})\right\rangle \\ &\qquad \times \left\langle \Psi^{M'}_3(\mathbf{r}',\boldsymbol{\rho}') \middle| \mathcal{G}(\mathbf{r}',\boldsymbol{\rho}') \phi^{f_{23}}_{\epsilon^*_{23}}(\mathbf{r}') e^{-i\mathbf{p}_{\rm mis}\cdot\boldsymbol{\rho}'} \lambda' \right\rangle. \end{aligned} \tag{50}$$

It is worth noticing that, in Eq. (46), the upper scripts $\frac{1}{2}\frac{1}{2}$ $(-\frac{1}{2}-\frac{1}{2})$ denote a nucleus polarized along (opposite) the quantization axis, while $\pm\frac{1}{2}\mp\frac{1}{2}$ indicate a nucleus polarized in the perpendicular (with regard to the quantization axis) plane, i.e., in our case, along the $x$ axis.

Let us consider first a longitudinally polarized nucleus; in this case, we have to consider in Eq. (46) only the terms with $M = M' = \pm 1/2$. One gets the following longitudinal contribution to the hadronic tensor:

$$\begin{aligned} W^{\parallel}_{\mu\nu}(\mathbf{S}_3, Q^2, P_h) &= \sum_{\lambda\lambda'} \sum_N \int d\mathbf{p}_{\rm mis} \int dE \frac{m_N}{E_N} \\ &\quad \times \left[\cos^2\frac{\beta}{2}\, \mathcal{P}^{N\,\frac{1}{2}\frac{1}{2}}_{\lambda\lambda'}\, w^{N\,\lambda\lambda'}_{\mu\nu} \right. \\ &\quad \left. + \sin^2\frac{\beta}{2}\, \mathcal{P}^{N\,-\frac{1}{2}-\frac{1}{2}}_{\lambda\lambda'}\, w^{N\,\lambda\lambda'}_{\mu\nu}\right]. \end{aligned} \tag{51}$$

In Eq. (51), $w_{\mu\nu}^{N\,\lambda\lambda'}$ is a short-hand notation for $w_{\mu\nu}^{N\,s.i.}(p_{\rm mis}, P_h, \lambda'\lambda)$, previously used. In the SIDIS process under investigation, since leptons are unpolarized, the leptonic tensor is symmetric and, as a consequence, only the symmetric part of the hadronic spin-dependent tensor, $w_{\mu\nu}^{sN\lambda\lambda'}$, is involved. For the diagonal terms of the symmetric part of the nucleon tensor (see, e.g., Ref. [3] for its general structure), one gets

$$\left\langle \tfrac{1}{2}\middle|\hat{w}_{\mu\nu}^{sN}\middle|\tfrac{1}{2}\right\rangle = -\left\langle -\tfrac{1}{2}\middle|\hat{w}_{\mu\nu}^{sN}\middle|-\tfrac{1}{2}\right\rangle, \tag{52}$$

while for the off-diagonal terms one has

$$\left\langle -\tfrac{1}{2}\middle|\hat{w}_{\mu\nu}^{sN}\middle|\tfrac{1}{2}\right\rangle = \left\langle \tfrac{1}{2}\middle|\hat{w}_{\mu\nu}^{sN}\middle|-\tfrac{1}{2}\right\rangle^{*}. \tag{53}$$

Then, making use of the properties under complex conjugation of the quantities (50), defined with respect to the quantization axis, namely

$$\tilde{\mathcal{O}}_{\lambda\lambda'}^{N\,MM'\,f_{23}}(E,\mathbf{p}_{\rm mis}) = (-1)^{M+M'+\lambda+\lambda'}\left[\tilde{\mathcal{O}}_{-\lambda-\lambda'}^{N\,-M-M'\,f_{23}}(E,\mathbf{p}_{\rm mis})\right]^{*}, \tag{54}$$

$$\tilde{\mathcal{O}}_{\lambda\lambda'}^{N\,MM'\,f_{23}}(E,\mathbf{p}_{\rm mis}) = \left[\tilde{\mathcal{O}}_{\lambda'\lambda}^{N\,M'M\,f_{23}}(E,\mathbf{p}_{\rm mis})\right]^{*}, \tag{55}$$

one obtains

$$W_{\mu\nu}^{||}(\mathbf{S}_3,Q^2,P_h) = \cos\beta \sum_N \int d\mathbf{p}_{\rm mis} \int dE \frac{m_N}{E_N}\left\{\left[\mathcal{P}_{\frac{1}{2}\frac{1}{2}}^{N\,\frac{1}{2}\frac{1}{2}} - \mathcal{P}_{-\frac{1}{2}-\frac{1}{2}}^{N\,\frac{1}{2}\frac{1}{2}}\right] w_{\mu\nu}^{sN\,\frac{1}{2}\frac{1}{2}} + \left[\mathcal{P}_{\frac{1}{2}-\frac{1}{2}}^{N\,\frac{1}{2}\frac{1}{2}}\, w_{\mu\nu}^{sN\,\frac{1}{2}-\frac{1}{2}} + \mathcal{P}_{-\frac{1}{2}\frac{1}{2}}^{N\,\frac{1}{2}\frac{1}{2}}\, w_{\mu\nu}^{sN\,-\frac{1}{2}\frac{1}{2}}\right]\right\}. \tag{56}$$

In Eq. (56), the first term in square brackets represents the *parallel* spin-dependent spectral function.

We are interested in single spin asymmetries measured with transversely polarized targets. The relevant hadronic tensor is therefore

$$\Delta W_{\mu\nu}^{s.i.}(\mathbf{S}_\perp,Q^2,P_h) = W_{\mu\nu}^{s.i.}(\mathbf{S}_3=\mathbf{S}_\perp,Q^2,P_h) - W_{\mu\nu}^{s.i.}(\mathbf{S}_3=-\mathbf{S}_\perp,Q^2,P_h), \tag{57}$$

where we choose $\mathbf{S}_\perp$ along the $x$ axis, i.e., $\beta = 90^\circ$. Then, using Eqs. (46) and (47), the quantity relevant to describe the JLab experiments turns out to be

$$\Delta W_{\mu\nu}^{s.i}(\mathbf{S}_\perp,Q^2,P_h) = W_{\mu\nu}^{\frac{1}{2}-\frac{1}{2}} + W_{\mu\nu}^{-\frac{1}{2}\frac{1}{2}}. \tag{58}$$

Therefore, we have to evaluate

$$\begin{aligned}\Delta W_{\mu\nu}^{s.i}(\mathbf{S}_3,Q^2,P_h) &= \sum_{\lambda\lambda'}\sum_N \int d\mathbf{p}_{\rm mis}\int dE\frac{m_N}{E_N}\left[\mathcal{P}_{\lambda\lambda'}^{N\,\frac{1}{2}-\frac{1}{2}}(E,\mathbf{p}_{\rm mis})\, w_{\mu\nu}^{Ns\lambda\lambda'} + \mathcal{P}_{\lambda\lambda'}^{N\,-\frac{1}{2}\frac{1}{2}}(E,\mathbf{p}_{\rm mis})\, w_{\mu\nu}^{Ns\lambda\lambda'}\right]\\ &= \sum_N \int d\mathbf{p}_{\rm mis}\int dE\frac{m_N}{E_N}\left\{\sum_\lambda\left[\mathcal{P}_{\lambda\lambda}^{N\,\frac{1}{2}-\frac{1}{2}}(E,\mathbf{p}_{\rm mis}) + \mathcal{P}_{\lambda\lambda}^{N\,-\frac{1}{2}\frac{1}{2}}(E,\mathbf{p}_{\rm mis})\right] w_{\mu\nu}^{sN\lambda\lambda}\right.\\ &\quad \left. + \sum_\lambda\left[\mathcal{P}_{\lambda-\lambda}^{N\,\frac{1}{2}-\frac{1}{2}}(E,\mathbf{p}_{\rm mis}) + \mathcal{P}_{\lambda-\lambda}^{N\,-\frac{1}{2}\frac{1}{2}}(E,\mathbf{p}_{\rm mis})\right] w_{\mu\nu}^{sN\lambda-\lambda}\right\}.\end{aligned} \tag{59}$$

One obtains, for the term in the last line of Eq. (59),

$$\begin{aligned}\sum_\lambda\left[\mathcal{P}_{\lambda-\lambda}^{N\,\frac{1}{2}-\frac{1}{2}}(E,\mathbf{p}_{\rm mis}) + \mathcal{P}_{\lambda-\lambda}^{N\,-\frac{1}{2}\frac{1}{2}}(E,\mathbf{p}_{\rm mis})\right] w_{\mu\nu}^{sN\lambda-\lambda} &= 2{\rm Re}\left\{\left[\mathcal{P}_{\frac{1}{2}-\frac{1}{2}}^{N\,\frac{1}{2}-\frac{1}{2}}(E,\mathbf{p}_{\rm mis}) + \mathcal{P}_{\frac{1}{2}-\frac{1}{2}}^{N\,-\frac{1}{2}\frac{1}{2}}(E,\mathbf{p}_{\rm mis})\right] w_{\mu\nu}^{sN\,\frac{1}{2}-\frac{1}{2}}\right\}\\ &= 2{\rm Re}\left[\mathcal{P}_{\frac{1}{2}-\frac{1}{2}}^{N\,\frac{1}{2}-\frac{1}{2}}(E,\mathbf{p}_{\rm mis}) + \mathcal{P}_{\frac{1}{2}-\frac{1}{2}}^{N\,-\frac{1}{2}\frac{1}{2}}(E,\mathbf{p}_{\rm mis})\right]{\rm Re}\left[w_{\mu\nu}^{sN\,\frac{1}{2}-\frac{1}{2}}\right]\\ &\quad - 2{\rm Im}\left[\mathcal{P}_{\frac{1}{2}-\frac{1}{2}}^{N\,\frac{1}{2}-\frac{1}{2}}(E,\mathbf{p}_{\rm mis}) + \mathcal{P}_{\frac{1}{2}-\frac{1}{2}}^{N\,-\frac{1}{2}\frac{1}{2}}(E,\mathbf{p}_{\rm mis})\right]{\rm Im}\left[w_{\mu\nu}^{sN\,\frac{1}{2}-\frac{1}{2}}\right],\end{aligned} \tag{60}$$

where the relations (53) and (55) have been used.

In Appendix B, it is shown that the contribution of the last line in Eq. (60) can be safely neglected, being of higher order in $\mathbf{p}_\perp/m_N$, where $\mathbf{p}_\perp$ is the nucleon transverse-momentum inside the target, with $\mathbf{p} = -\mathbf{p}_{\rm mis}$. Besides, in the remaining expression, only the zero-order term in $\mathbf{p}_\perp/m_N$ yields a sizable contribution. Hence, $\mathbf{p}_\perp$ does not give relevant contributions to the hadronic tensor, and the expression of the nucleon hadronic tensor obtained in a collinear frame, where $\mathbf{p}_\perp = \mathbf{0}$, for example, the one given in Ref. [3] for the Collins process (cf. Sec. 6.5), can be safely used. As a consequence, the final expression for the nuclear hadronic tensor, suitable for calculations of SSAs, reads

$$\Delta W_{\mu\nu}^{s.i}(\mathbf{S}_3,Q^2,P_h) = \sum_N \int d\mathbf{p}_{\rm mis}\int dE\frac{m_N}{E_N}\left\{\mathcal{P}^{N\,\perp}(E,\mathbf{p}_{\rm mis}) w_{\mu\nu}^{N\perp} + 2,[\mathcal{P}^{N\,(\perp-||)}(E,\mathbf{p}_{\rm mis})] w_{\mu\nu}^{sN\,\frac{1}{2}\frac{1}{2}}\right\}, \tag{61}$$

where Eqs. (52) and (54) have been used to obtain the last term.

In Eq. (61), the transverse spectral function has been introduced

$$\mathcal{P}^{N\perp}(E,\mathbf{p}_{\rm mis}) = {\rm Re}\Big[\mathcal{P}^{N\,\frac{1}{2}-\frac{1}{2}}_{\frac{1}{2}-\frac{1}{2}}(E,\mathbf{p}_{\rm mis}) + \mathcal{P}^{N\,-\frac{1}{2}+\frac{1}{2}}_{\frac{1}{2}-\frac{1}{2}}(E,\mathbf{p}_{\rm mis})\Big], \tag{62}$$

and the quantity

$$w^{N\perp}_{\mu\nu} \equiv \Big[w^{sN\,\frac{1}{2}-\frac{1}{2}}_{\mu\nu} + w^{sN\,-\frac{1}{2}\frac{1}{2}}_{\mu\nu}\Big] \tag{63}$$

has been defined. Furthermore, in Eq. (61), the transverse-longitudinal spectral function,

$$\mathcal{P}^{N(\perp-||)}(E,\mathbf{p}_{\rm mis}) = \mathcal{P}^{N\,\frac{1}{2}-\frac{1}{2}}_{\frac{1}{2}\frac{1}{2}}(E,\mathbf{p}_{\rm mis}) + \mathcal{P}^{N\,-\frac{1}{2}\frac{1}{2}}_{\frac{1}{2}\frac{1}{2}}(E,\mathbf{p}_{\rm mis}), \tag{64}$$

is a real quantity which represents, in PWIA, the probability distribution to find a longitudinally polarized nucleon minus the probability distribution to have a nucleon polarized in the direction opposite to the $z$ axis in a transversely polarized nucleus. It should be pointed out that, in PWIA, the transverse spectral function $\mathcal{P}^{N\perp}(E,\mathbf{p}_{\rm mis})$ yields the probability distribution to find a nucleon polarized along the $x$ axis minus the probability distribution to find a nucleon polarized against the $x$ axis in a transversely polarized nucleus with a polarization vector $\mathbf{S}_3$ along the $x$ axis.

For the nuclear cross section, Eq. (44), one gets

$$\sigma^3(\mathbf{S}_3) = \sum_N \int d\mathbf{p}_{\rm mis} \int dE \frac{\tilde{\alpha} m_N}{E_N} [\sigma^{N\perp}\mathcal{P}^{N\perp}(E,\mathbf{p}_{\rm mis}) + \sigma^{N||}\mathcal{P}^{N(\perp-||)}(E,\mathbf{p}_{\rm mis})], \tag{65}$$

where $\sigma^{N\perp}$ and $\sigma^{N||}$ are the cross sections, Eq. (19), for transversely and longitudinally polarized nucleons, respectively.

Note also that, when FSI are included, the quantities corresponding to the PWIA parallel spectral function, $P^{N||}$, Eq. (14), and the PWIA perpendicular spectral function, $P^{N\perp}$, Eq. (15), are different, due to the eikonal direction which breaks the rotational invariance of the problem.

## V. THE COLLINS AND SIVERS ASYMMETRIES FOR $^3$He

As discussed in the introduction, a series of SIDIS experiments are planned at JLab, using a transversely polarized $^3$He target and an unpolarized electron beam, detecting a fast pion (kaon) in the final state. The Sivers and Collins SSAs of $^3$He will be therefore measured, with the aim of extracting the corresponding neutron quantities. The formal results of the present approach for the $^3$He SSAs, and for the extraction of the neutron information, are presented in this section.

The Sivers and Collins asymmetries are defined through proper moments of the experimental SIDIS cross sections, viz.,

$$A_3^{\rm Col(Siv)} \equiv \frac{\int d\phi_{S_3} d\phi_h \sin(\phi_h \pm \phi_{S_3})[\sigma^3(\mathbf{S}_3,\phi_h,\phi_{S_3},z) - \sigma^3(\mathbf{S}_3,\phi_h,\phi_{S_3}+\pi,z)]}{\int d\phi_h \sigma^3_{\rm unpol}(x_{Bj},Q^2,\mathbf{P}_h)}, \tag{66}$$

where $\phi_h$ is the azimuthal angle between the hadron and the lepton planes, $\phi_{S_3}$ is the azimuthal angle between the target polarization and the lepton plane according to the conventions fixed in Ref. [48], and $z = E_h/\nu$ is the fraction of energy transfer carried by the detected meson. Inserting the cross section Eq. (65) in the above equation, one gets

$$A_3^{\rm Col(Siv)} = \frac{\int_{x_{Bj}}^3 d\alpha\Big[\Delta\sigma^n_{\rm Col(Siv)}(x_{Bj}/\alpha,Q^2,z) f_n^{\perp,i}(\alpha,Q^2,\mathcal{E}) + 2\Delta\sigma^p_{\rm Col(Siv)}(x_{Bj}/\alpha,Q^2,z) f_p^{\perp,i}(\alpha,Q^2,\mathcal{E})\Big]}{\int d\alpha\Big[\sigma^n(x_{Bj}/\alpha,Q^2,z) f_n^i(\alpha,Q^2,\mathcal{E}) + 2\sigma^p(x_{Bj}/\alpha,Q^2,z) f_p^i(\alpha,Q^2,\mathcal{E})\Big]}, \tag{67}$$

where $\mathcal{E}$ is the energy of the incoming lepton [see below Eq. (1)] and $f^{\perp,i}_{p(n)}(\alpha,Q^2,\mathcal{E})$ are the light-cone momentum distributions of transversely polarized nucleons in a transversely polarized nucleus for $i$ = PWIA or FSI. One defines

$$f_N^{\perp,i}(\alpha,Q^2,\mathcal{E}) = \int_{E_{\rm min}}^{E_{\rm max}} dE f_N^{\perp,i}(\alpha,Q^2,\mathcal{E},E), \tag{68}$$

where

$$f_N^{\perp,i}(\alpha,Q^2,\mathcal{E},E) = \int d\mathbf{p}_{\rm mis} \frac{m_N}{E_N} \mathcal{P}^{N\perp,i}(E,\mathbf{p}_{\rm mis}) \delta\left(\alpha + \frac{\tilde{p}_{\rm mis}\cdot q}{m_N \nu}\right) \theta\big[W_Y^2 - (m_N+m_\pi)^2\big], \tag{69}$$

with $W_Y$ being the invariant mass of the debris $Y$ that hadronizes in a nucleon and at least one pseudoscalar meson. For the sake of definiteness, in Eq. (69) and in what follows we consider a $\pi^-$ in the final state. Let us recall that in the unpolarized case, the light-cone momentum distributions read

$$f_N^i(\alpha,Q^2,\mathcal{E}) = \int_{E_{\rm min}}^{E_{\rm max}} dE f_N^i(\alpha,Q^2,\mathcal{E},E), \tag{70}$$

with

$$f_N^i(\alpha,Q^2,\mathcal{E},E)=\int d\mathbf{p}_{\rm mis}\frac{m_N}{E_N}\mathcal{P}^{Ni}(E,\mathbf{p}_{\rm mis})\delta\left(\alpha+\frac{\tilde{p}_{\rm mis}\cdot q}{m_N\nu}\right)\theta\left[W_Y^2-(m_N+m_\pi)^2\right], \tag{71}$$

where $\mathcal{P}^{Ni}(E,\mathbf{p}_{\rm mis})=\sum_\lambda \mathcal{P}^{Ni}_{\lambda\lambda}$. In Eqs. (69) and (71), the $\delta$ function can be eliminated by integrating over the angle between $\mathbf{p}_{\rm mis}$ and $\mathbf{q}$; the limits of integration on $|\mathbf{p}_{\rm mis}|$, i.e., $|\mathbf{p}_{\rm min}|$ and $|\mathbf{p}_{\rm max}|$, and on $E$, $E_{\rm min}$, and $E_{\rm max}$, are determined from the condition $|\cos\theta_{pq}|\leqslant 1$ and from the requirement $W_Y^2\geqslant(m_N+m_\pi)^2$, since we consider SIDIS with at least one pion in the final state. As a consequence, $|\mathbf{p}_{\rm min}|$ and $|\mathbf{p}_{\rm max}|$ are functions of $\alpha,E,Q^2,\mathcal{E}$. One should notice that, in the Bjorken limit, they would be functions of $\alpha$ and $E$ only. In Eqs. (68) and (70), one has $E_{\rm min}=B_3-B_2\sim 5.5$ MeV.

Moreover, as explained in the previous section, one can obtain the distributions for the two cases, $i=$ PWIA, FSI, just substituting, in the same equations, the corresponding spectral functions $\mathcal{P}^{Ni}(E,\mathbf{p}_{\rm mis})$ and $\mathcal{P}^{N\perp i}(E,\mathbf{p}_{\rm mis})$. The evaluation of $\mathcal{P}^{Ni}(E,\mathbf{p}_{\rm mis})$, when both the nuclear structure and the effects of FSI are included, is the main technical achievement of this paper. Actual numerical results, based on (i) two- and three-nucleon wave functions [49] evaluated with the nucleon-nucleon AV18 interaction [32] and (ii) the GEA mechanism, are discussed in detail in the following section. In what follows, when the distorted spectral functions will be considered in Eqs. (69) and (71), we will call the distribution functions in Eqs. (68) and (70) *distorted light-cone momentum distributions* (see Appendix B).

In Eq. (66), one should notice that, after multiplying the nuclear hadronic tensor by $\sin(\phi_{S_3}\pm\phi_h)$ and integrating over $\phi_{S_3}$, the transverse-longitudinal term in Eq. (65) does not contribute to the numerators in the asymmetries above defined, due to the properties of the spin-dependent SIDIS nucleon tensor [4].

In Eq. (67), the quantities $\Delta\sigma^N_{\rm Col(Siv)}$ and $\sigma^N$, related to the structure of the bound nucleon, are defined as follows (see, e.g., Ref. [4]):

$$\Delta\sigma^N_{Col}(x_{Bj},Q^2,z)=\frac{1-y}{1-y+y^2/2}\sum_q e_q^2\int d^2\boldsymbol{\kappa}_T d^2\mathbf{k}_T\delta^2(\mathbf{k}_T+\mathbf{q}_T-\boldsymbol{\kappa}_T)\frac{\hat{\mathbf{P}}_{h\perp}\cdot\boldsymbol{\kappa}_T}{m_h}h_1^{q,N}\left(x_{Bj},\mathbf{k}_T^2\right)H_1^{\perp q,h}[z,(z\boldsymbol{\kappa}_T)^2], \tag{72}$$

$$\Delta\sigma^N_{Siv}(x_{Bj},Q^2,z)=\sum_q e_q^2\int d^2\boldsymbol{\kappa}_T d^2\mathbf{k}_T\delta^2(\mathbf{k}_T+\mathbf{q}_T-\boldsymbol{\kappa}_T)\frac{\hat{\mathbf{P}}_{h\perp}\cdot\mathbf{k}_T}{m_N}f_{1T}^{\perp q,N}\left(x_{Bj},\mathbf{k}_T^2\right)D_1^{q,h}[z,(z\boldsymbol{\kappa}_T)^2], \tag{73}$$

$$\sigma^N(x_{Bj},Q^2,z)=\sum_q e_q^2\int d^2\boldsymbol{\kappa}_T d^2\mathbf{k}_T\delta^2(\mathbf{k}_T+\mathbf{q}_T-\boldsymbol{\kappa}_T)f_1^{q,N}\left(x_{Bj},\mathbf{k}_T^2\right)D_1^{q,h}[z,(z\boldsymbol{\kappa}_T)^2]. \tag{74}$$

In the last three equations, the quantities $\mathbf{k}_T$ and $\boldsymbol{\kappa}_T$ are the intrinsic transverse momenta of the parton in the bound nucleon and in the produced hadron, respectively; following the notation of SIDIS, a subscript $T$ means transverse with respect to $\mathbf{P}_h$ (the three-momentum of the final pion or kaon), while the subscript $\perp$ means transverse with respect to $\mathbf{q}$. The transverse momentum-dependent parton distributions, $h_1^{q,N}(x_{Bj},\mathbf{k}_T^2)$, $f_{1T}^{\perp q,N}(x_{Bj},\mathbf{k}_T^2)$, $f_1^{q,N}(x_{Bj},\mathbf{k}_T^2)$, and the transverse momentum-dependent fragmentation functions, $D_1^{q,h}[z,(z\boldsymbol{\kappa}_T)^2]$, $H_1^{\perp q,h}[z,(z\boldsymbol{\kappa}_T)^2]$, appearing in Eqs. (72), (73), and (74), have been evaluated using experimental data whenever possible, or using proper model estimates. One should realize that the main goal of the present study is the estimate of nuclear effects in the extraction of the neutron information, rather than obtaining absolute predictions on the SSAs of $^3$He, which would be affected anyhow by the poor present knowledge of some of the distributions necessary to perform the actual calculation. Any reasonable choice of the distribution functions of the nucleon is therefore suitable for our study. In particular, in the actual calculations, we have made use of the same functions adopted in Ref. [31]:

(1) For the unpolarized parton distribution, $f_1^{q,N}(x_{Bj})$, the parametrization of Ref. [50], with a Gaussian ansatz for the $\mathbf{k}_T$ dependence, has been used.
(2) For the transversity distribution, $h_1^{q,N}$, the ansatz $h_1=g_1$ has been used; i.e., the transversity distribution has been taken to be equal to the helicity distribution. This gives certainly the correct order of magnitude. In particular, the parametrization of Ref. [51] has been used.
(3) For the Sivers function, $f_{1T}^{\perp q}(x_{Bj},\mathbf{k}_T^2)$ in Eq. (73), the fit proposed in Ref. [52] has ben adopted.
(4) For the unpolarized fragmentation function $D_1^{q,h}(z)$, different models are used for evaluating the Sivers and Collins asymmetries. In particular, for the Sivers asymmetry, the parametrization in Ref. [53] has been used, while for the Collins one, the model calculation of Ref. [54] has been adopted (see Ref. [31] for details);
(5) For the basically unknown Collins fragmentation function, $H_1^{\perp q}[z,(z\boldsymbol{\kappa}_T)^2]$, appearing in Eq. (72), the model calculation of Ref. [54] has been used.

Because of the nuclear binding, nucleons are off shell. However, in our approach, the parton structure of the nucleons are parameterized using parton distributions of free nucleons. In principle, medium modifications of the structure functions, in addition to the ones due to conventional nuclear effects, could be implemented. For example, one could think to apply a method similar to the one used in Ref. [55] to study off-shell effects in the evaluation of inclusive polarized structure functions $g_{1,2}$ of

$^3$He. In that paper, a dependence of the polarized structure functions $g_{1,2}$ for the nucleons on the off-shell mass $p^2$ was introduced, with a further integration on $p^2$ in the convolutions. The quantitative effect of this procedure would be in any case difficult to establish, due to the necessary use of ingredients, such as the off-shell structure functions, experimentally unknown and difficult to constrain theoretically. An analysis of this kind is beyond the goal of the present paper.

If one would like to consider the SIDIS hadronic tensor at an higher twist level, then other (higher twist) TMDs, at the moment completely unknown experimentally, would be involved. At the nuclear level, this would imply the appearance of other combinations of matrix elements of the spectral function. While these ingredients should be under control, since any overlap with any nuclear or nucleon relative polarization is at hand, the evaluation of the asymmetries would be strongly affected by the ignorance on the nucleon part. Therefore, for the moment we prefer to give results at a basic level in this first study of the effects of FSI in polarized SIDIS processes.

Equation (67) has been presented in Ref. [31] within PWIA. As already noticed, within GEA the theoretical expression of the nuclear asymmetries does not formally change in presence of FSI. Therefore, Eq. (67) can be exploited also in this case, but using the suitable ingredient, i.e., the distorted spin-dependent spectral function, and eventually evaluating the distorted light-cone momentum distributions.

Let us discuss now the crucial issue of the extraction of the neutron information from $^3$He data. A strategy for extracting the neutron Sivers and Collins asymmetries from $^3$He data, developed in Ref. [31], is summarized and applied in the following.

If the results of the calculation were able to simulate $^3$He data, the problem would amount to unfolding the convolution formula. This can be done taking into account that the light-cone momentum distributions $f_N(\alpha,Q^2,\mathcal{E})$ and $f_N^\perp(\alpha,Q^2,\mathcal{E})$ exhibit sharp maxima at $\alpha\sim 1$, i.e., $f_N(\alpha,Q^2,\mathcal{E})\sim\delta(\alpha-1)$ even in presence of FSI, as we will show in the next section. Let us recall that this peak is expected since $\alpha=-(\tilde{p}_{\rm mis}\cdot q)/m_N\nu$ plays the role of the Bjorken variable for a bound nucleon. Assuming that the $\delta$-like behavior for the light-cone distributions is a reliable approximation (as shown in what follows), then $\Delta\sigma^n_{\rm Col(Siv)}(x_{Bj}/\alpha,Q^2,\mathbf{S}^n_\perp,z)\sim\Delta\sigma^n_{\rm Col(Siv)}(x_{Bj},Q^2,\mathbf{S}^n_\perp,z)$, and the calculated asymmetries $A_3$ can be written as (notably, the dependence on $\mathcal{E}$ becomes milder approaching the Bjorken limit)

$$A_3^{\rm Col(Siv)}\simeq\frac{\Delta\sigma_3^{\rm Col(Siv)}}{\sigma}\simeq\frac{\Delta\sigma^n_{\rm Col(Siv)}(x_{Bj},Q^2,\mathbf{S}^n_\perp,z)\int d\alpha f_n^\perp(\alpha,Q^2)+2\Delta\sigma^p_{\rm Col(Siv)}(x_{Bj},Q^2,\mathbf{S}^n_\perp,z)\int d\alpha f_p^\perp(\alpha,Q^2)}{\sigma^n(x_{Bj},Q^2,z)\int d\alpha f_n(\alpha,Q^2)+2\sigma^p(x_{Bj},Q^2,z)\int d\alpha f_p(\alpha,Q^2)}. \tag{75}$$

Let us introduce the so-called dilution factors as

$$d_{p(n)}(x_{Bj},z)=\frac{\sigma^{p(n)}(x_{Bj},Q^2,z)}{\langle N_n\rangle\sigma^n(x_{Bj},Q^2,z)+2\langle N_p\rangle\sigma^p(x_{Bj},Q^2,z)}, \tag{76}$$

where

$$\langle N_{p(n)}\rangle=\int_{E_{\rm min}}^{E_{\rm max}}dE\int d\mathbf{p}_{\rm mis}\,\mathcal{P}^{p(n)}(E,\mathbf{p}_{\rm mis})\theta\big[W_Y^2-(m_{p(n)}+m_\pi)^2\big], \tag{77}$$

Notice that within PWIA and in the Bjorken limit, when $W_Y\to\infty$, then $\langle N_{p(n)}\rangle$ must strictly be 1, providing an obvious physical meaning. In the presence of FSI, there is a depletion that spoils the above interpretation in terms of number of nucleons involved in the elementary process.

By using the dilution factors, Eq. (75) can be approximated as follows:

$$A_{^3{\rm He}}^{\rm Col(Siv)}\simeq p_n^\perp\,d_n A_n^{\rm Col(Siv)}+2\,p_p^\perp\,d_p A_p^{\rm Col(Siv)}, \tag{78}$$

where $A^{\rm Col(Siv)}_{n(p)}$ are the free nucleon asymmetries and $p^\perp_{n(p)}$ are the average, or effective, transverse polarizations of the neutron (proton) in a transversely polarized $^3$He nucleus, given by

$$p^\perp_{p(n)}=\int_{E_{\rm min}}^{E_{\rm max}}dE\int d\mathbf{p}_{\rm mis}\,\mathcal{P}^{p(n)\perp}(E,\mathbf{p}_{\rm mis})\theta\big[W_Y^2-(m_{p(n)}+m_\pi)^2\big]. \tag{79}$$

In the Bjorken limit, they are $Q^2$ independent and can be obtained directly from the nuclear wave function, without evaluating the complicated final states entering the spectral function. In such a limit, by adopting the nucleon-nucleon AV18 interaction and disregarding relativistic corrections (see Ref. [41]) one gets that the effective longitudinal and transverse polarizations coincide and are equal to

$$p_n^\perp=p_n^{||}=p_n\simeq 0.878,\quad p_p^\perp=p_p^{||}=p_p\simeq -0.024.$$

It is important to stress that, using another realistic potential, these values change by a few percent at most [20]. We also note that, to obtain Eq. (78), the term $m_N/E_N$ in the definition of the light cone momentum distibutions $f_N^\perp$, Eq. (68), and $f_N$, Eq. (70), has been neglected in Eq. (75). We checked that this procedure introduces a change in the nuclear asymmetries of the order of a few parts in one thousand, which is not relevant phenomenologically.

The free nucleon asymmetries $A_N^{\mathrm{Col(Siv)}}$ can be calculated in terms of the quark distributions and fragmentation functions previously described, using their leading twist definitions [4]:

$$A_N^{\mathrm{Col}} = \frac{1-y}{1-y+y^2/2} \frac{\sum_q e_q^2 \int d^2\boldsymbol{\kappa}_T d^2\mathbf{k}_T \delta^2(\mathbf{k}_T+\mathbf{q}_T-\boldsymbol{\kappa}_T)(\hat{\mathbf{P}}_{\mathbf{h}\perp}\cdot\boldsymbol{\kappa}_T/m_h) h_1^{q,N}\left(x_{Bj},\mathbf{k}_T^2\right) H_1^{\perp q,h}(z,(z\boldsymbol{\kappa}_T)^2)}{\sum_q e_q^2 \int d^2\boldsymbol{\kappa}_T d^2\mathbf{k}_T \delta^2(\mathbf{k}_T+\mathbf{q}_T-\boldsymbol{\kappa}_T) f_1^{q,N}\left(x_{Bj},\mathbf{k}_T^2\right) D_1^{q,h}[z,(z\boldsymbol{\kappa}_T)^2]}, \tag{80}$$

and

$$A_N^{\mathrm{Siv}} = \frac{\sum_q e_q^2 \int d^2\boldsymbol{\kappa}_T d^2\mathbf{k}_T \delta^2(\mathbf{k}_T+\mathbf{q}_T-\boldsymbol{\kappa}_T)(\hat{\mathbf{P}}_{h\perp}\cdot\mathbf{k}_T/m_N) f_{1T}^{\perp q,N}\left(x_{Bj},\mathbf{k}_T^2\right) D_1^{q,h}(z,(z\boldsymbol{\kappa}_T)^2)}{\sum_q e_q^2 \int d^2\boldsymbol{\kappa}_T d^2\mathbf{k}_T \delta^2(\mathbf{k}_T+\mathbf{q}_T-\boldsymbol{\kappa}_T) f_1^{q,N}\left(x_{Bj},\mathbf{k}_T^2\right) D_1^{q,h}[z,(z\boldsymbol{\kappa}_T)^2]}. \tag{81}$$

If Eq. (78) were a good approximation of reality, it would be possible to use it to extract the neutron asymmetry according to the following recipe, suggested in Ref. [15] for the polarized DIS case, and in Ref. [31] for polarized SIDIS in PWIA and in the Bjorken limit (for $j$ = Collins, Sivers):

$$A_n^j \simeq \frac{1}{p_n d_n}\left(A_3^{\exp,j} - 2p_p d_p A_p^{\exp,j}\right). \tag{82}$$

A theoretical check of Eq. (82) can be performed if a realistic calculation of the $^3$He single spin asymmetries, $A_3^{\mathrm{theo},j}$, is introduced in Eq. (82) in place of the forthcoming experimental data $A_3^{\exp,j}$, and models for $A_p^{\exp,j}$ and $A_n^j$ are used in the theoretical calculation of $A_3^{\mathrm{theo},j}$ and in the right-hand side of the above equation. If nuclear effects were safely taken care of by Eq. (78), one should be able to extract, according to Eq. (82), the neutron asymmetry used as an input for calculating $A_3^{\mathrm{theo},j}$. Namely, a self-consistency check can be carried out, in preparation of the future extraction from the experimental $A_3^{\exp,j}$. It has to be noticed that a more stringent test of Eq. (82) could be attained if SSAs of $^3$H will become available at some time in the future (let us recall that some steps forward in the actual use of unpolarized $^3$H target in DIS experiments have been accomplished [39]).

## VI. RESULTS AND DISCUSSION

Now we are ready to present the results of our calculation.

Let us start by providing a pictorial view of the main quantity of interest, i.e., the distorted spectral function, evaluated using $^3$He and $\Psi_{23}$ wave functions computed within the AV18 potential [32]. As an example, the neutron spectral function, in the unpolarized case, is shown in Fig. 2, in PWIA and with FSI between debris and spectator taken into account, within the GEA framework. It is clearly seen that, as found in previous studies dedicated to quasielastic scattering [45], the effect of FSI increases with $\mathbf{p}_{\mathrm{mis}}$, as it is easily understood by thinking that, when $\mathbf{p}_{\mathrm{mis}} = \mathbf{p}_Y - \mathbf{q}$ is low, the final debris $Y$ has to be very fast. The low impact of FSI for small values of $|\mathbf{p}_{\mathrm{mis}}|$ is illustrated in more detail in Fig. 3, where it is shown the ratio of the unpolarized distorted spectral function of the neutron, evaluated for $\alpha = 1$, to the PWIA one. Also, the increase of the relevance of FSI when, at fixed $|\mathbf{p}_{\mathrm{mis}}|$, the removal energy $E = M_{23}^* + m_N - M_3$ increases, is physically expected. As a matter of fact, from the energy conservation

$$M_3 + \nu = \sqrt{M_{23}^{*2} + |\mathbf{p}_{\mathrm{mis}}|^2} + \sqrt{M_Y^2 + |\mathbf{p}_Y|^2} \tag{83}$$

with $M_Y \geqslant m_\pi + m_N$, one can realize that the momentum $|\mathbf{p}_Y|$ has to decrease (i) for any $|\mathbf{p}_{\mathrm{mis}}|$, when the removal energy increases, and (ii) for any $\epsilon_{23}^*$, when $|\mathbf{p}_{\mathrm{mis}}|$ increases. Then, the debris gets slower and FSI sizably affects the distorted spectral function. This is indeed what can be seen in Fig. 3.

The results for the spin-independent and spin-dependent light-cone momentum distributions have already been evaluated and shown in Ref. [31], in PWIA, using the AV18 interaction [32], but assuming the Bjorken limit ($|\vec{q}| \simeq \nu$). Let us perform a first step forward, by illustrating in Figs. 4 and 5 the effect of JLab kinematics, at finite values of $\nu$ and $Q^2$, on the light-cone momentum distributions (68) and (70), using the PWIA spectral function already exploited in Ref. [31]. As already mentioned, in the kinematics under scrutiny, the dis-

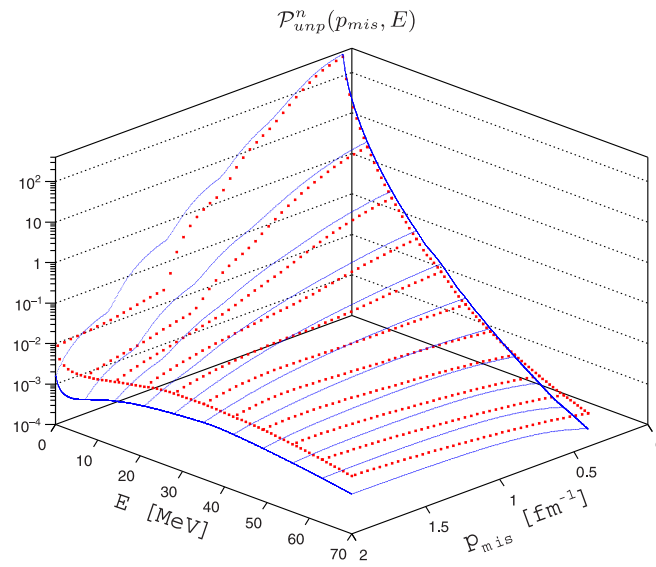


FIG. 2. The $^3$He spectral function, for the neutron, in the unpolarized case, as a function of $p_{\mathrm{mis}} = |\mathbf{p}_{\mathrm{mis}}|$ and of the removal energy $E$, in PWIA (full lines) and with FSI taken into account within GEA framework (dotted lines), The kinematical ranges of $p_{\mathrm{mis}}$ and $E$ correspond to the ones relevant for the calculation of the unpolarized light-cone distribution for $\alpha = 1$, $\mathcal{E} = 11$ GeV [cf. Eq. (71)], $x_{Bj} = 0.48$, and $Q^2 = 7.6$ GeV$^2$.

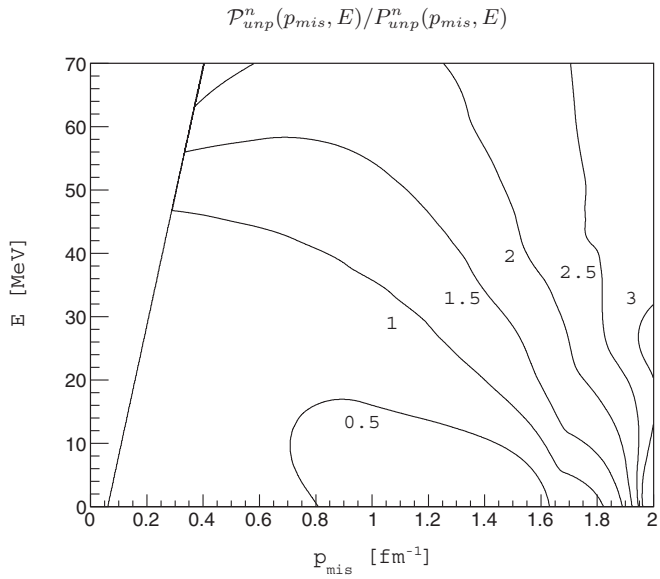


FIG. 3. The ratio between the unpolarized neutron spectral function with FSI interactions and the corresponding quantity in PWIA that are shown in Fig. 2.

tribution functions $f_{n(p)}(\alpha,Q^2,\mathcal{E})$ and $f^{\perp}_{n(p)}(\alpha,Q^2,\mathcal{E})$ depend on both the energy $\nu$ and the momentum $\mathbf{q}$ through the limits of integration $|\mathbf{p}_{\min(\max)}|$ and the invariant mass of the debris. Figure 4 shows $|\mathbf{p}_{\min}|$ and $|\mathbf{p}_{\max}|$ as a function of the light-cone variable $\alpha$, for two values of the removal energy $E$, i.e., $E = 0$ and 200 MeV, given the electron beam energy, $\mathcal{E} = 8.8$ GeV, and $Q^2 = 5.73(\mathrm{GeV/c})^2$. For this kinematical choice, it is seen that one can explore only the region where $\alpha \geqslant 0.55$ (i.e., when $|\mathbf{p}_{\max}| > |\mathbf{p}_{\min}|$). By changing the kinematics, one can investigate a wider interval of $\alpha$. Figure 5, where the PWIA distribution function $f_N(\alpha,Q^2,\mathcal{E})$ and $f^{\perp}_N(\alpha,Q^2,\mathcal{E})$ are

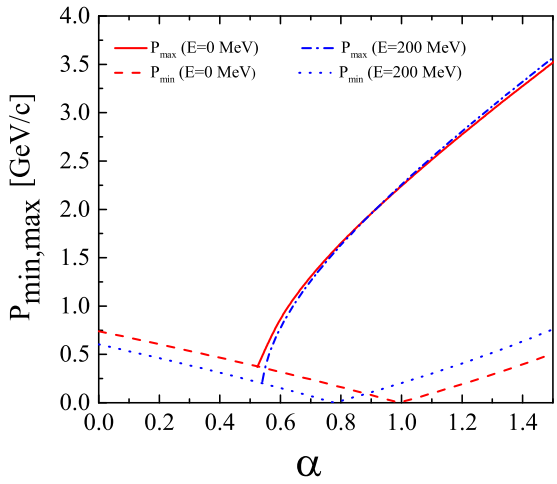


FIG. 4. Dependence on $\alpha$ of the integration limits $p_{\min,\max} = |\mathbf{p}_{\min,\max}|$ in Eqs. (69) and (71) for the 3bbu channel and two values of the removal energy $E$, in the kinematics of the forthcoming JLab experiments (corresponding to an initial electron energy $\mathcal{E} = 8.8$ GeV).

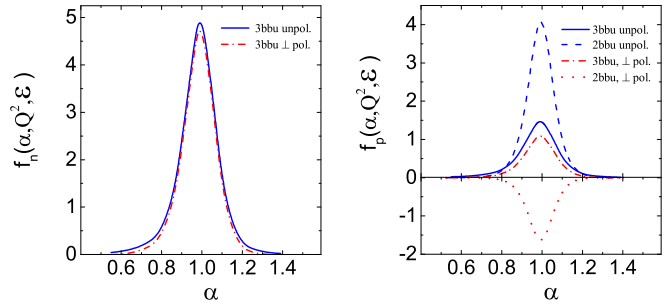


FIG. 5. The PWIA distribution functions $f^{\perp}_N(\alpha,Q^2,\mathcal{E})$, Eq. (68), and $f_N(\alpha,Q^2,\mathcal{E})$, Eq. (70), for the neutron (left panel) and the proton (right panel) at $\mathcal{E} = 8.8$ GeV, and $Q^2 = 5.73(\mathrm{GeV/c})^2$. For the polarized proton, in the 2bbu and 3bbu channels, these distributions are almost equal and opposite in sign, resulting in a very small total distribution.

presented for the above kinematical conditions, shows that, as happens in the Bjorken limit, the polarization of the $^3$He nucleus is almost entirely determined by the neutron one, while the contribution of the proton polarization is very small. It is worth mentioning that the existence of a kinematically forbidden region $\alpha < 0.55$ can lead to slight modifications in the normalization conditions for both the unpolarized and the polarized light-cone momentum distributions.

In Fig. 6, the investigation on the PWIA light-cone distributions becomes more detailed. The functions $f^{\perp}_{n(p)}(\alpha,Q^2,\mathcal{E},E)$ and $f_{n(p)}(\alpha,Q^2,\mathcal{E},E)$ of Eqs. (69) and (71), respectively, are shown for two different choices of kinematics, corresponding to the planned experiments at JLab, and $\alpha = 0.65$. Such a value of $\alpha$ belongs to the region where the neutron light-cone momentum distributions (unpolarized and transversely polarized) have shown the biggest differences in PWIA. In correspondence with the different kinematical choices, the calculated curves are hardly distinguishable and one can conclude that the dependence upon kinematics is rather mild in PWIA.

The extraction procedure shown in Eq. (82) and proposed in Ref. [31] for SIDIS adopting PWIA and Bjorken limit works very well and it has been already applied in the experimental analysis of the JLab data collected at 6 GeV [29]. In the actual JLab kinematics, a nontrivial $Q^2$ dependence is introduced in the integration limits of the convolution formula (cf. Fig. 4). This amounts to a deviation of the quantities $\langle N_n\rangle$, $\langle N_p\rangle$, $p_n$, $p_p$ from their values obtained in the Bjorken limit, namely 1, 1, 0.878, $-0.024$, respectively. In the kinematics of JLab at 12 GeV [23], this deviation is found to be a few parts in one thousand. In Fig. 7, it is shown that the excellent performance of the extraction procedure of Eq. (82) does not change appreciably when we move from the Bjorken limit to the experimental kinematics of JLab at 12 GeV [23], corresponding to finite values of $Q^2$ and $\nu \neq |\vec{q}|$. Hence, the Sivers (left panel) and the Collins (right panel) asymmetries are well determined when our theoretical check of Eq. (82) is carried out.

Now comes the basic issue of understanding to what extent FSI effects between debris and remnants can modify the

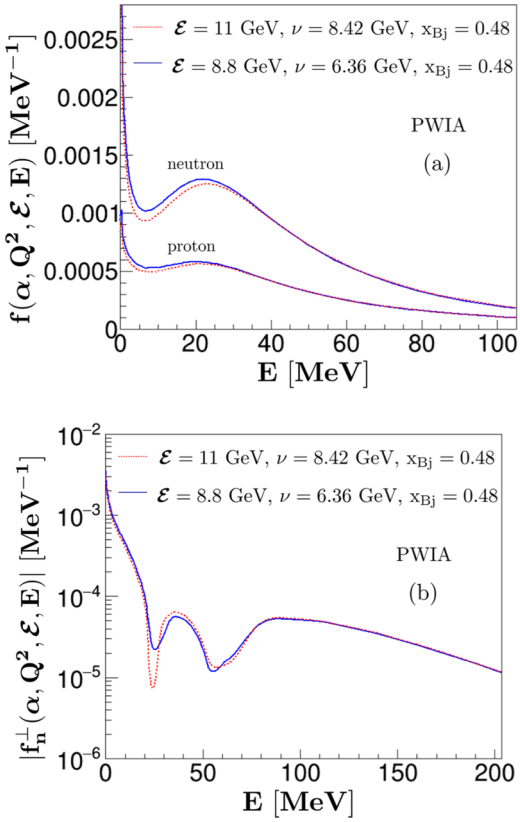


FIG. 6. The functions $f_N(\alpha = 0.65, Q^2, \mathcal{E}, E)$ and $f_N^\perp(\alpha = 0.65, Q^2, \mathcal{E}, E)$, Eqs. (71) and (69) respectively, evaluated in PWIA, for the following kinematics: (1) $\mathcal{E} = 11$ GeV and $Q^2 = 7.58$ (GeV/c)$^2$ (dashed lines); (2) $\mathcal{E} = 8.8$ GeV, and $Q^2 = 5.73$ (GeV/c)$^2$ (solid lines). (a) The proton and neutron functions $f_N(\alpha = 0.65, Q^2, \mathcal{E}, E)$ in an unpolarized $^3$He. (b) The functions $f_N^\perp(\alpha = 0.65, Q^2, \mathcal{E}, E)$ for a transversely polarized neutron in a transversely polarized $^3$He. For a transversely polarized proton, the corresponding function, very small, is not shown.

outcomes obtained through Eq. (82) and shown in Fig. 7. This is a crucial step for a reliable extraction of the neutron information. As pointed out in Secs. III, IV, and V, the formal expressions for the Collins and Sivers asymmetries obtained within PWIA, Eq. (67), still work when FSI are considered within GEA.

Also Eqs. (68)–(70) remain formally unchanged if FSI are included: The only difference amounts to use there the distorted spectral function for obtaining the distorted light-cone momentum distributions, instead of adopting the corresponding PWIA expressions. In Figs. 8 and 9, neutron and proton light-cone momentum distributions, obtained within GEA for the unpolarized and the transversely polarized cases, are shown for $\mathcal{E} = 8.8$ GeV, a value of the beam energy typical for the planned JLab@12 experiments, and for $Q^2 = 5.73$ (GeV/c)$^2$ (i.e., one of the values which will be tested at $\mathcal{E} = 8.8$ GeV). Moreover, they are compared with the corresponding quantities calculated within PWIA. The differences between the results with and without FSI are quite sizable and therefore the quantities defined in Eqs. (72), (73), and (74), necessary to calculate Collins and Sivers asymmetries, are

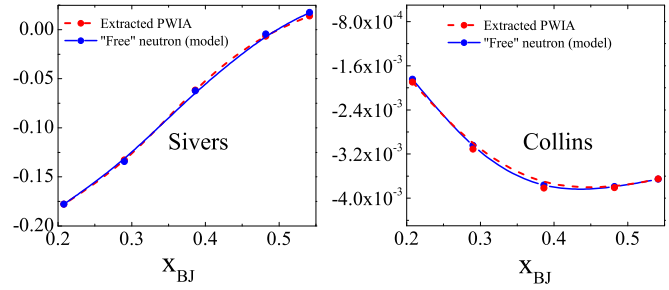


FIG. 7. The neutron Sivers (left panel) and Collins (right panel) asymmetries for the JLab kinematics at an initial electron energy of $\mathcal{E} = 8.8$ GeV. Full line, the model for the neutron asymmetry used in the calculation; dashed line, the neutron asymmetry extracted from the PWIA calculation using Eq. (82). Calculations have been performed at $Q^2 = 5.73$ (GeV/c)$^2$, i.e., the central $Q^2$ value for an energy beam $\mathcal{E} = 8.8$ GeV (see text).

largely affected by FSI effects, have to be carefully taken into account. In particular, $\langle N_n \rangle$, $\langle N_p \rangle$, $p_n$, $p_p$, defined according to Eqs. (77) and (79), respectively, and calculated at the actual JLab kinematics corresponding to $Q^2 \sim 3 \div 7$ (GeV/c)$^2$, are affected by FSI and exhibit deviations from their values in the Bjorken limit (given above) as large as 20%.

The $Q^2$ dependence of the above results is quite important, in view of the possible construction of the EIC (see, e.g., Ref. [56] for the presentation of the physics case) that could open unprecedented possibilities in the studies of the nucleon TMDs. In order to give an idea of the impact on the future measurements, Fig. 10 shows the ratio of the light-cone spin-independent momentum distribution, evaluated taking into account FSI, to the corresponding quantity obtained in PWIA, for different values of $Q^2$ at the peak, i.e., $\alpha = 1$. Four different kinematical conditions have been chosen, and two of them, namely (i) $\mathcal{E} = 8.8$ GeV, $Q^2 \simeq 5.7$ (GeV/c)$^2$, $x_{Bj} \simeq 0.48$ and (ii) $\mathcal{E} = 11$ GeV, $Q^2 \simeq 7.7$ (GeV/c)$^2$, $x_{Bj} \simeq 0.48$, are typical for JLab@12. The third and the fourth ones are kinematics occurring at the planned EIC, namely at $\mathcal{E}_{\text{collider}} = 11$ GeV, $\mathcal{E}^{^3\text{He}}_{\text{collider}} = 40$ GeV, $Q^2 = 10$ and 12 (GeV/c)$^2$, $x_{Bj} \simeq 0.48$ (note that this value of $x_{Bj}$ could be achieved by a beam energy $\mathcal{E} = 293$ GeV for a fixed target experiment). It is important to

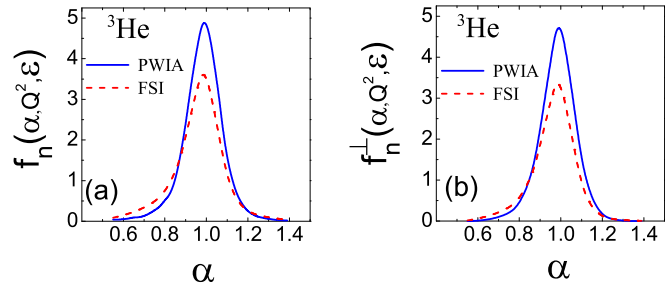


FIG. 8. The neutron unpolarized (a) and transversely polarized (b) distributions, Eqs. (70) and (68). Solid lines are PWIA results, while dashed lines include effects of FSI. JLab kinematics has been assumed, i.e., the initial electron energy is $\mathcal{E} = 8.8$ GeV and $Q^2 = 5.73$ (GeV/c)$^2$, which is the central $Q^2$ value for an energy beam $\mathcal{E} = 8.8$ GeV (see text).

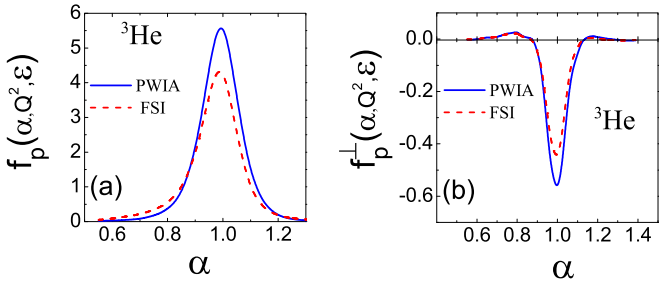


FIG. 9. The same as in Fig. 8, but for the proton distributions.

recall that a single point in Fig. 10 represents the outcome of a one-week run on the ZEFIRO INFN facility in Pisa, Italy. What is found is that the effects of FSI, evaluated within GEA framework, is almost $Q^2$ independent but rather sizable at JLab and EIC energies. Could one think that the extraction procedure shown in Eq. (82) had to be abandoned in favor of more involved and model-dependent techniques? Actually, a crucial observation is now in order. It is clearly seen in Figs. 5, 8, and 9 that the spin-independent and spin-dependent light-cone momentum distributions are strongly peaked around $\alpha = 1$, both in PWIA and with FSI effects taken into account. This means that the approximation given in Eq. (75) for the nuclear Sivers and Collins asymmetries [cf. Eq. (67)] should basically hold. Moreover, looking at the same figures, it is also rather apparent that FSI produces a decrease of all the distributions in a similar way, both qualitatively and quantitatively. From Eq. (75), it is easy to see that the results for the nuclear asymmetries obtained in PWIA, $A_3^{\mathrm{PWIA},j}$, or taking into account FSI, $A_3^{\mathrm{FSI},j}$ (recall that $j =$ Sivers or Collins), should not sizably differ from each other, due to a cancellation of effects present in both the numerator and

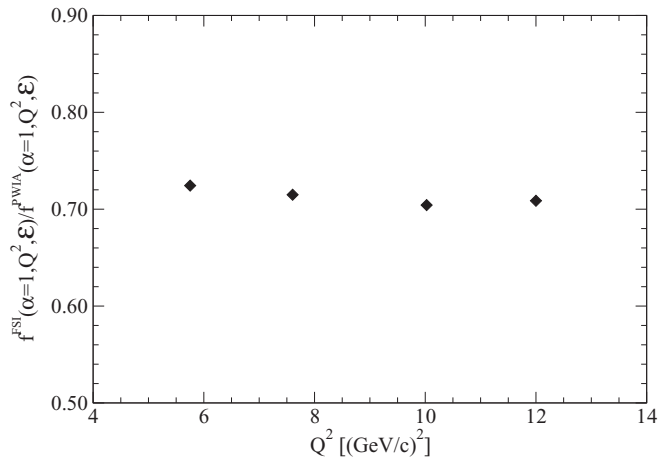


FIG. 10. The ratio of the light-cone spin-independent momentum distribution evaluated taking into account FSI to the corresponding quantity obtained in PWIA. The ratio is shown in the neutron case, for $\alpha = 1$, namely the value where the distributions reach their maximum value, as a function of the momentum transfer, $Q^2$, corresponding to four different kinematical conditions: the ones with $Q^2 < 9$ (GeV/c)$^2$ have been evaluated by using JLab kinematical conditions, while the rightmost diamonds are appropriate for EIC kinematics (see text).

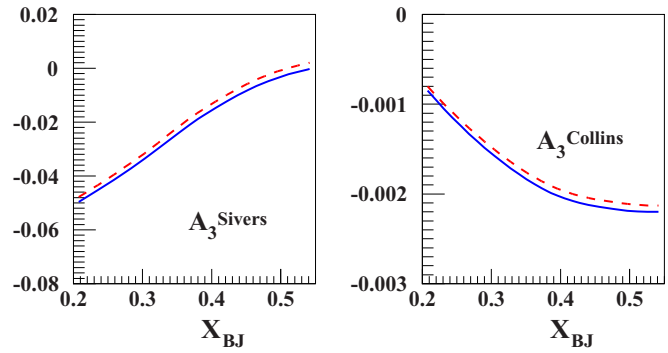


FIG. 11. Left panel: The $^3$He Sivers asymmetry [see Eqs. (67) and (73)], evaluated taking into account FSI effects (full line) and in PWIA (dashed line). Right panel: the same, but for the $^3$He Collins asymmetry [see Eqs. (67) and (72)]. Calculations have been performed at $Q^2 = 5.73$ (GeV/c)$^2$, i.e., the central $Q^2$ value for an energy beam $\mathcal{E} = 8.8$ GeV (see text).

the denominator. The realization of this fact in the actual calculation of Eq. (67) is shown in Fig. 11. In principle, in this figure and in the two following ones, any $x_{Bj}$ should correspond to a slightly different value of $Q^2$. Nevertheless, in the $x_{Bj}$ range explored at fixed $\mathcal{E}$, the dependence on $Q^2$ of the light-cone momentum distributions $f_{p(n)}(\alpha, Q^2, \mathcal{E})$ and $f^\perp_{p(n)}(\alpha, Q^2, \mathcal{E})$ is rather mild and therefore we will show the results for the nuclear asymmetries, Eq. (67), at a fixed value of $Q^2$, namely 5.73 (GeV/c)$^2$.

Our full evaluations of the $^3$He Collins and Sivers asymmetries, presented in Fig. 11, strongly encourage the investigation of the extraction formula, Eq. (82), that relies on the validity of the approximation Eq. (78), where effective polarization *and* dilution factors are multiplied by each other. In particular, we want to assess if Eq. (82) can be safely (or better with a low degree of uncertainty) applied to the experimental data, where FSI is certainly acting. The relevant product of effective polarizations and dilution factors is found to have a very little dependence on FSI, as one can straightforwardly realize by

TABLE I. The PWIA values of the dilution factors $d_{n(p)}(x_{Bj},z)$ and their product with the corresponding effective polarizations, in PWIA, for the kinematical conditions of the planned experiments at JLab, with scattering angle $\theta_e = 30^\circ$ and detected pion angle $\theta_\pi = 14^\circ$. The effective polarizations are evaluated with extrema of integrations depending upon the kinematics. At $Q^2 = 5.73$ (GeV/c)$^2$, i.e., the central $Q^2$ value for an energy beam $\mathcal{E} = 8.8$ GeV, one obtains $p_n = 0.876$, $p_p = -0.024$ [cf. Eq. (79)], very close to the corresponding asymptotic values 0.878 and $-0.024$ (i.e., in the Bjorken limit).

| $\mathcal{E}$ (GeV) | $x_{Bj}$ | $\nu$ (GeV) | $P_\pi$ (GeV/c) | $d_n(x_{Bj},z)$ | $p_n d_n$ | $d_p(x_{Bj},z)$ | $p_p d_p$ |
|---|---|---|---|---|---|---|---|
| 8.8 | 0.21 | 7.55 | 3.40 | 0.304 | 0.266 | 0.348 | $-8.4 \times 10^{-3}$ |
| 8.8 | 0.29 | 7.15 | 3.19 | 0.286 | 0.251 | 0.357 | $-8.5 \times 10^{-3}$ |
| 8.8 | 0.48 | 6.36 | 2.77 | 0.257 | 0.225 | 0.372 | $-8.9 \times 10^{-3}$ |
| 11 | 0.21 | 9.68 | 4.29 | 0.302 | 0.265 | 0.349 | $-8.3 \times 10^{-3}$ |
| 11 | 0.29 | 9.28 | 4.11 | 0.285 | 0.250 | 0.357 | $-8.5 \times 10^{-3}$ |

TABLE II. The same as in Table I, but taking into account FSI within GEA framework. For all the presented kinematical conditions, one gets *distorted polarizations*, evaluated by using Eq. (79), with distorted distributions. They amount to $p_n \simeq 0.756$, $p_p \simeq -0.0265$ for $Q^2 = 5.73$ (GeV/c)$^2$, i.e., the central $Q^2$ value for an energy beam $\mathcal{E} = 8.8$ GeV. In these conditions one gets, for the quantities $\langle N_n \rangle$ and $\langle N_p \rangle$, Eq. (77), the values 0.85 and 0.87, respectively.

| $\mathcal{E}$ (GeV) | $x_{Bj}$ | $\nu$ (GeV) | $P_\pi$ (GeV/c) | $d_n(x_{Bj},z)$ | $p_n d_n$ | $d_p(x_{Bj},z)$ | $p_p d_p$ |
|---|---|---|---|---|---|---|---|
| 8.8 | 0.21 | 7.55 | 3.40 | 0.353 | 0.267 | 0.405 | $-1.1 \times 10^{-2}$ |
| 8.8 | 0.29 | 7.15 | 3.19 | 0.332 | 0.251 | 0.415 | $-1.1 \times 10^{-2}$ |
| 8.8 | 0.48 | 6.36 | 2.77 | 0.298 | 0.225 | 0.432 | $-1.2 \times 10^{-2}$ |
| 11 | 0.21 | 9.68 | 4.29 | 0.351 | 0.266 | 0.405 | $-1.0 \times 10^{-2}$ |
| 11 | 0.29 | 9.28 | 4.11 | 0.331 | 0.250 | 0.415 | $-1.1 \times 10^{-2}$ |

inspecting Tables I and II, where the dilution factors, effective polarizations, and their products are presented with or without FSI effects taken into account, by adopting the kinematics of the forthcoming JLab experiments.

Considering that (i) $A_3^{\mathrm{PWIA},j} \simeq A_3^{\mathrm{FSI},j}$ (see Fig. 11) and (ii) the products of effective polarizations and dilution factors are almost the same in PWIA and including FSI, one has

$$A_n^j \simeq \frac{1}{p_n^{\mathrm{PWIA}} d_n^{\mathrm{PWIA}}} \left( A_3^{\mathrm{PWIA},j} - 2 p_p^{\mathrm{PWIA}} d_p^{\mathrm{PWIA}} A_p^{\exp,j} \right) \simeq \frac{1}{p_n^{\mathrm{FSI}} d_n^{\mathrm{FSI}}} \left( A_3^{\mathrm{FSI},j} - 2 p_p^{\mathrm{FSI}} d_p^{\mathrm{FSI}} A_p^{\exp,j} \right). \quad (84)$$

In Fig. 12, the reliability of the above relations in the extraction of $A_n^j$ is illustrated through our theoretical test, where the experimental $A_3^{\exp,j}$ is replaced by our full calculation. Indeed, in Fig. 12, the model Collins and Sivers asymmetries for the neutron used in the full calculations of $^3$He asymmetries are hardly distinguishable from the neutron asymmetries extracted through Eq. (84) by using PWIA effective polarizations and

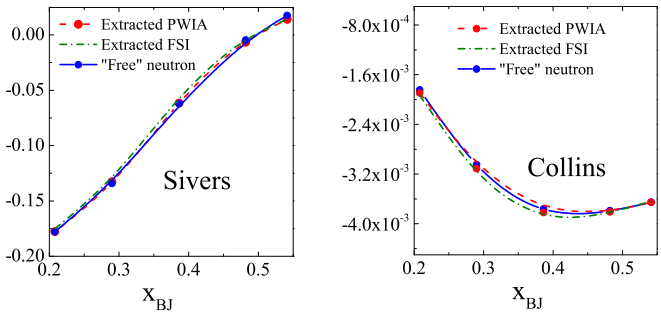


FIG. 12. The neutron Sivers (left panel) and Collins (right panel) asymmetries for the JLab kinematics at an initial electron energy of $\mathcal{E} = 8.8$ GeV. Full line, the model for the neutron asymmetry used in the calculation; dot-dashed line, the neutron asymmetry extracted from the full calculation of $A_3^j$ with FSI taken into account, using the extraction formula Eq. (84); dashed line, the result obtained using Eq. (84) to extract the neutron asymmetries from PWIA results. Calculations have been performed at $Q^2 = 5.73$ (GeV/c)$^2$, i.e., the central $Q^2$ value for an energy beam $\mathcal{E} = 8.8$ GeV (see text).

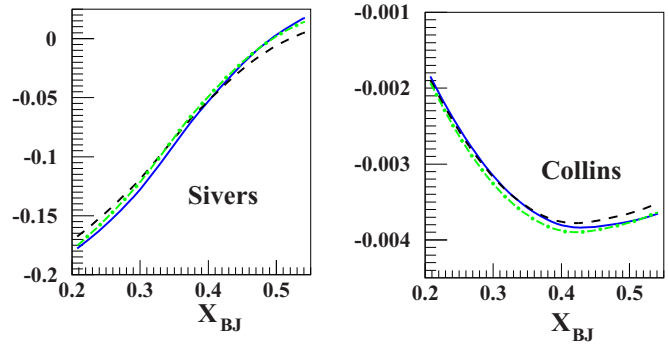


FIG. 13. The neutron Sivers (left panel) and Collins (right panel) asymmetries, for the JLab kinematics at an initial electron energy of $\mathcal{E} = 8.8$ GeV. Full line, the model for the neutron asymmetry used in the calculation; dot-dashed line, the neutron asymmetry extracted from the full calculation of $A_3^j$ with FSI taken into account, using the extraction formula Eq. (84); dashed line, the result obtained using Eq. (85) to extract the neutron asymmetries from the same calculation. Calculations have been performed at $Q^2 = 5.73$ (GeV/c)$^2$, i.e., the central $Q^2$ value for an energy beam $\mathcal{E} = 8.8$ GeV (see text).

dilution factors, or by considering the corresponding quantities calculated within GEA (a preliminary version of this figure was presented in Ref. [57]). It should be pointed out that these quantities can be evaluated in any kinematical configuration using our model of FSI, which is rather well constrained phenomenologically and could be improved checking our predictions against the spin-dependent cross sections which will be soon available.

In addition to the above extraction procedure, one could adopt the following one where the experimental inputs are $A_3^{\exp,j}$ and $A_p^{\exp,j}$, while the theoretical quantities reduce to the PWIA effective polarization in the Bjorken limit. In this case, one has a nice possibility to extract the neutron information through another extraction scheme, independent of the FSI model. The procedure is based on the following expression:

$$A_n^j \simeq \frac{1}{p_n^{\mathrm{PWIA}} d_n^{\exp}} \left( A_3^{\exp,j} - 2 p_p^{\mathrm{PWIA}} d_p^{\exp} A_p^{\exp,j} \right). \quad (85)$$

Indeed, $p_{n(p)}^{\mathrm{PWIA}}$ can be obtained from a realistic wave function with very small model dependence (see Ref. [20] for an analysis of the dependence of effective polarizations on different realistic potentials). In Eq. (85), the experimental dilution factors are

$$d_{p(n)}^{\exp}(x_{Bj},Q^2,z) = \frac{\sigma^{p(n)}(x_{Bj},Q^2,z)}{\sigma^n(x_{Bj},Q^2,z) + 2\sigma^p(x_{Bj},Q^2,z)}, \quad (86)$$

where no dependence on the FSI model is present, unlike Eq. (76). In Fig. 13, one sees that the uncertainty in the extraction procedure based on Eq. (85) is not much bigger than the one occurred by using Eq. (84). In Fig. 13, Eq. (85) has been actually evaluated using $A_3^{\mathrm{FSI},j}$ instead of $A_3^{\exp,j}$, and using, instead of $d_{p(n)}^{\exp}$, the dilution factors evaluated with the parametrizations of unpolarized parton distributions [50] and fragmentation functions [53] already described in the previous section. Therefore, Fig. 13 shows that, for a

safe extraction procedure through Eq. (85), the evaluation of distorted effective polarizations and dilution factors, which appear in Eq. (84) and depend on the adopted FSI model, is actually not required.

In summary, the comparisons shown in Figs. 12 and 13 illustrate two methods for the successful extraction of the neutron single spin asymmetries using transversely polarized $^3$He targets at JLab, and they represent the most relevant outcomes of the present investigation.

One could argue that the very nice results obtained within our FSI model are actually expected to hold in any description of final state interactions which is (i) factorized and (ii) basically spin independent, i.e., producing a similar effect in spin-dependent and spin-independent cross sections. This last feature is very likely to be realized for any FSI occurring in processes where the relative energy of the interacting systems is high, as is the case in the present study.

Indeed, the differential cross section $(d\sigma/dt)_{el}$ decreases exponentially with the momentum transfer $|t|$ and is essentially located at low momentum transfer $|t|$, i.e., in the forward direction. A thorough analysis of the spin dependence of the nucleon-nucleon cross section, in terms of the analyzing power $A_N$, can be found, e.g., in Refs. [58] and [59], where the shape dependence of $A_N$ in $|t|$ is studied, with particular attention to the region where the interference terms of the electromagnetic and nuclear interactions are important. As a result, $A_N$ is of a few percent at most and goes to zero as $|t|$ goes to zero. Consequently, only the central part of the amplitude contributes to the integrated cross section.

## VII. CONCLUSIONS

Measurements of the Sivers and Collins asymmetries for both proton and deuteron have shown a strong flavor dependence, motivating independent further investigations using different targets to safely access the same quantities for the neutron. As for any polarized neutron observable, $^3$He is the natural target, due to its specific spin structure. Two experiments, aimed at measuring azimuthal asymmetries in the production of $\pi^{\pm}$ from transversely polarized $^3$He, were performed at JLab. From the gathered $^3$He data [29], the Collins and Sivers neutron asymmetries were extracted using a procedure proposed in Ref. [31]. However, such an extraction procedure did not consider some relevant nuclear effects, properly evaluated in the present paper, which strengthens *a posteriori* the method used in Ref. [29] to obtain the neutron information. In particular, the extraction procedure proposed in Ref. [31] and used in Ref. [29] was able to take care of (i) the spin structure of $^3$He and (ii) the momentum and energy distributions of bound nucleons, through a realistic spin-dependent spectral function evaluated by using nuclear wave functions obtained from the AV18 interaction, in plane wave impulse approximation. The results of Ref. [31] were obtained in the Bjorken limit, namely without considering possible effects of the kinematics of JLab, dominated by finite values of the energy and momentum transfers, and, more important, without FSI effects. The problem of whether the extraction procedure based on PWIA calculations can be extended to a scenario where final state interactions between the debris, originated from the struck nucleon, and the interacting spectator system are allowed to play a role, as it likely happens in the actual JLab kinematics, has been thoroughly analyzed in the present paper. We were able to quantitatively show that the extraction procedure is basically independent of FSI, evaluated within the generalized eikonal approximation. In particular, in order to perform the needed full evaluation of the FSI effects, we have extended the calculation of a realistic distorted spin-dependent spectral function, introduced in a previous paper of ours [38], where we took into account the two-body break up channel only. Actually, we have performed a highly nontrivial (from the numerical point of view) computation of the contribution to the distorted spin-dependent spectral function from the three-body breakup channel, essential to obtain reliable cross sections and in turn to robustly extract valuable neutron information. Once such a refined spectral function became available, we have exploited our results for calculating both Sivers and Collins single spin asymmetries. FSI effects have been found to produce sizable effects in both the unpolarized and polarized cross sections. On the contrary, the SSAs are only slightly affected by FSI, since they are ratios of cross sections, and therefore the FSI effects cancel to a large extent. As a result, the very same extraction procedure proven to be successful in PWIA can be used also in a scenario where FSI effects are relevant. This means that all the complexities related to Fermi motion, binding, and FSI effects can be summarized in the nucleon effective polarizations, quantities known from accurate few-body calculations in a rather model-independent way. This scheme is valid in a wide range of FSI models, every time that FSI are basically spin independent (see the end of previous section), as expected to happen at high energies (i.e., in the case of JLab or the planned Electron Ion Collider) and lead to convolution formulas for the nuclear cross sections, namely a folding of cross sections off bound nucleons and distorted spin-dependent spectral functions.

To test our model for the FSI, we plan to compare our results with the very recent unpolarized SIDIS cross sections from a $^3$He target of Ref. [46]. A more stringent test of our model would require a comparison with measurements of SIDIS cross sections off a polarized $^3$He target, since polarization experiments can be more sensitive to FSI effects. It would be particularly interesting to investigate the kinematical regions where FSI effects are expected to be more relevant [38].

The importance of these results for both the planning and the analysis of experiments with transversely polarized $^3$He target is clear. Further studies of the same issue will involve the implementation of GEA in the relativistic nuclear overlaps, defined in Ref. [41], so that a light-front, distorted, spin-dependent spectral function can be evaluated and relativistic effects can be taken into account in a consistent framework.

## ACKNOWLEDGMENTS

Calculations were in part performed on the ZEFIRO facility of INFN, Commissione 4, Pisa, Italy. L.P.K. thanks INFN, Perugia, for partial financial support during his stay in Perugia in 2015 and 2016, and the Dipartimento di Fisica e Geologia of Perugia University for warm hospitality.

## APPENDIX A: OVERLAPS FOR THE DISTORTED SPECTRAL FUNCTION

The overlaps

$$\tilde{\mathcal{O}}^{N\,M\,M'}_{\lambda\lambda'}(\epsilon^*_{23},\mathbf{p}_{\rm mis}) = \left\langle \lambda,\tau^N,\phi_{\epsilon^*_{23}}(\mathbf{r})e^{-i\mathbf{p}_{\rm mis}\boldsymbol{\rho}}\mathcal{G}(\mathbf{r},\boldsymbol{\rho})\right|\left.\Psi^M_3(\mathbf{r},\boldsymbol{\rho})\right\rangle\left\langle\Psi^{M'}_3(\mathbf{r}',\boldsymbol{\rho}')\right|\left.\lambda',\tau^N,\mathcal{G}(\mathbf{r}',\boldsymbol{\rho}')\phi_{\epsilon^*_{23}}(\mathbf{r}')e^{-i\mathbf{p}_{\rm mis}\boldsymbol{\rho}'}\right\rangle, \tag{A1}$$

corresponding to Eq. (50) with the index $f_{23}$ removed for simplicity, are built in terms of two- and three-body wave functions.

In particular, when the energy of the pair is $\epsilon^*_{23} = t^2/m$, the two-body wave function reads

$$\phi^{\mathbf{t}}_{s_{23}\sigma_{23}T_{23}\tau_{23}}(\mathbf{r}) = 4\pi \sum_{lml_f J_f M_f} \langle lms_{23}\sigma_{23}|J_f M_f\rangle Y^*_{lm}(\hat{\mathbf{t}})i^l \psi^{J_f}_{ll_f s_{23}}(|\mathbf{t}|,|\mathbf{r}|)Y^{l_f s_{23}}_{J_f M_f}(\hat{\mathbf{r}})|T_{23}\tau_{23}\rangle, \tag{A2}$$

with the tensor spherical harmonics defined as

$$Y^{l_f s_{23}}_{J_f M_f}(\hat{\mathbf{r}}) = \sum_{m_f\sigma'_{23}} \langle l_f m_f s_{23}\sigma'_{23}|J_f M_f\rangle Y_{l_f m_f}(\hat{\mathbf{r}})\chi_{s_{23}\sigma'_{23}}. \tag{A3}$$

When the pair is in the deuteron state, with binding energy $E_D$, the two-body wave function reads

$$\phi_{M_D}(E_D,\mathbf{r}) = u_0(r)Y^{01}_{1M_D}(\hat{\mathbf{r}}) + u_2(r)Y^{21}_{1M_D}(\hat{\mathbf{r}}). \tag{A4}$$

The three-body wave function in Ref. [49] is defined according to the following scheme:

$$\begin{aligned}\left\langle \sigma_1,\sigma_2,\sigma_3;T_{23},\tau_{23},\tau;\boldsymbol{\rho},\mathbf{r}\right|^3\mathrm{He};\frac{1}{2}M\frac{1}{2}T_z\Big\rangle &= \left\langle T_{23}\tau_{23}\frac{1}{2}\tau\left|\frac{1}{2}T_z\right\rangle\sum_{L_\rho M_\rho}\sum_{XM_X}\sum_{j_{23}m_{23}}\left\langle XM_XL_\rho M_\rho\left|\frac{1}{2}M\right\rangle\right\langle j_{23}m_{23}\frac{1}{2}\sigma_1\right|XM_X\right\rangle\\ &\times\sum_{s_{23}\sigma_{23}}\sum_{l_{23}\mu_{23}}\left\langle\frac{1}{2}\sigma_2\frac{1}{2}\sigma_3|s_{23}\sigma_{23}\right\rangle\langle l_{23}\mu_{23}s_{23}\sigma_{23}|j_{23}m_{23}\rangle Y_{l_{23}\mu_{23}}(\hat{\mathbf{r}})\\ &\times Y_{L_\rho M_\rho}(\hat{\boldsymbol{\rho}})\phi^{j_{23}l_{23}s_{23}}_{L_\rho X}(|\mathbf{r}|,|\boldsymbol{\rho}|).\end{aligned} \tag{A5}$$

The antisymmetrization of the wave function requires $l_{23}+s_{23}+T_{23}$, where $T_{23}$ is the isospin of the pair 23, to be odd. In addition, $l_{23}+L_\rho$ has to be even, due to the parity of $^3$He.

Using these wave functions, one has, in the 3bbu channel,

$$\begin{aligned}\sum_{\sigma_{23}T_{23}\tau_{23}}\int d\hat{\mathbf{t}}\,\tilde{\mathcal{O}}^{N\,M\,M'}_{\lambda\lambda'}(\epsilon^*_{23},\mathbf{p}_{mis}) &= \sum_{\sigma_{23}\tilde{\sigma}_{23}}\sum_{\{\alpha,\tilde{\alpha}\}}\sum_{l\,J_f M_f}\sum_{M_X\tilde{M}_X m_{23}\tilde{m}_{23}}\left\langle XM_XL_\rho M_\rho|\frac{1}{2}M\right\rangle\left\langle\tilde{X}\tilde{M}_X\tilde{L}_\rho\tilde{M}_\rho|\frac{1}{2}M'\right\rangle\\ &\times\left\langle j_{23}m_{23}\frac{1}{2}\lambda|XM_X\right\rangle\left\langle\tilde{j}_{23}\tilde{m}_{23}\frac{1}{2}\lambda'|\tilde{X}\tilde{M}_X\right\rangle\langle l_{23}\mu_{23}s_{23}\sigma_{23}|j_{23}m_{23}\rangle\langle\tilde{l}_{23}\tilde{\mu}_{23}s_{23}\tilde{\sigma}_{23}|\tilde{j}_{23}\tilde{m}_{23}\rangle\\ &\times\langle l_f m_f s_{23}\sigma_{23}|J_f M_f\rangle\langle\tilde{l}_f\tilde{m}_f s_{23}\tilde{\sigma}_{23}|J_f M_f\rangle\,O^{(FSI)}_{\{\alpha\}lJ_f s_{23}}(\epsilon^*_{23},\mathbf{p}_{mis})\,O^{(FSI)}_{\{\tilde{\alpha}\}lJ_f s_{23}}(\epsilon^*_{23},\mathbf{p}_{mis}),\end{aligned} \tag{A6}$$

where $\{\alpha\} = \{L_\rho,M_\rho,X,j_{23},l_f,m_f,l_{23},\mu_{23}\}$ and

$$O^{(FSI)}_{\{\alpha\}lJ_f s_{23}}(\epsilon^*_{23},\mathbf{p}_{mis}) = 4\pi\int d\boldsymbol{\rho}\int d\mathbf{r}\,e^{i\mathbf{p}_{mis}\cdot\boldsymbol{\rho}}\mathcal{G}(\mathbf{r},\boldsymbol{\rho})\psi^{J_f\,*}_{ll_f s_{23}}(|\mathbf{t}|,|\mathbf{r}|)\,Y^*_{l_f m_f}(\hat{\mathbf{r}})\,Y_{L_\rho M_\rho}(\hat{\boldsymbol{\rho}})Y_{l_{23}\mu_{23}}(\hat{\mathbf{r}}),\phi^{j_{23}l_{23}s_{23}}_{L_\rho X}(|\mathbf{r}|,|\boldsymbol{\rho}|). \tag{A7}$$

When the active nucleon $N$ is a proton $p$, besides the 3*bbu* channel, one can have also the 2bbu channel, for which the overlap becomes

$$\begin{aligned}\sum_{M_D}\mathcal{O}^{N=p\,M\,M'}_{\lambda\lambda'}(E_D,\mathbf{p}_{\rm mis}) &= \sum_{M_D M_X\tilde{M}_X m_{23}\tilde{m}_{23}\sigma_{23}\tilde{\sigma}_{23}}\\ &\times\sum_{\{\beta,\tilde{\beta}\}}\left\langle XM_XL_\rho M_\rho|\frac{1}{2}M\right\rangle\left\langle\tilde{X}\tilde{M}_X\tilde{L}_\rho\tilde{M}_\rho|\frac{1}{2}M'\right\rangle\left\langle j_{23}m_{23}\frac{1}{2}\lambda|XM_X\right\rangle\left\langle\tilde{j}_{23}\tilde{m}_{23}\frac{1}{2}\lambda'|\tilde{X}\tilde{M}_X\right\rangle\\ &\times\langle\,l_{23}\mu_{23}1\sigma_{23}|j_{23}m_{23}\,\rangle\langle\,\tilde{l}_{23}\tilde{\mu}_{23}1\tilde{\sigma}_{23}|\tilde{j}_{23}\tilde{m}_{23}\,\rangle\langle\,L_D m_L 1\sigma_{23}|1M_D\,\rangle\\ &\times\langle\,\tilde{L}_D\tilde{m}_L 1\tilde{\sigma}_{23}|1M_D\,\rangle\,O^{(FSI)}_{\beta}(E_D,\mathbf{p}_{\rm mis})O^{(FSI)}_{\tilde{\beta}}(E_D,\mathbf{p}_{\rm mis}),\end{aligned} \tag{A8}$$

where

$$O^{(FSI)}_{\beta}(E_D,\mathbf{p}_{\rm mis}) = \int d\boldsymbol{\rho}\int d\mathbf{r}\,e^{i\mathbf{p}_{\rm mis}\boldsymbol{\rho}}\mathcal{G}(\mathbf{r},\boldsymbol{\rho})u_{L_D}(|\mathbf{r}|)Y^*_{L_D m_L}(\hat{\mathbf{r}})Y_{L_\rho M_\rho}(\hat{\boldsymbol{\rho}})Y_{l_{23}\mu_{23}}(\hat{\mathbf{r}})\phi^{j_{23}L_D 1}_{L_\rho X}(|\mathbf{r}|,|\boldsymbol{\rho}|), \tag{A9}$$

and $\{\beta\} = \{L_\rho,M_\rho,X,j_{23},l_{23},\mu_{23},L_D=0,2,m_L\}$.

## APPENDIX B: PROPERTIES OF THE GLAUBER DISTORTED SPECTRAL FUNCTION

Let us consider a reference frame with the $z$ axis along the momentum transfer $\mathbf{q}$. If in such a reference frame a nucleus with $J_A = 1/2$ has a polarization $\mathbf{S}_A$, one can expand the nucleus state by using pure states polarized with respect to the quantization axis $\hat{q} \equiv \hat{e}_z$, i.e., $|\frac{1}{2}, \pm\frac{1}{2}\rangle_{\hat{q}}$. In this case, a generic state with $J_A = 1/2$ and polarization directed along some direction is written as follows:

$$\left|\frac{1}{2},\frac{1}{2}\right\rangle_{\hat{S}_A} = \cos\frac{\beta}{2}\left|\frac{1}{2},\frac{1}{2}\right\rangle_{\hat{q}} + \sin\frac{\beta}{2}\left|\frac{1}{2},-\frac{1}{2}\right\rangle_{\hat{q}}, \tag{B1}$$

where $\cos\beta = \hat{S}_A \cdot \hat{q}$ and $|\frac{1}{2},\frac{1}{2}\rangle_{\hat{S}_A}$ is a pure state polarized with respect to the quantization axis $\hat{S}_A$ [see Eq. (43)]. In Eq. (19) of Ref. [19], one can find a general expression of the PWIA spectral function,

$$\boldsymbol{P}_{\mathcal{M}}(\mathbf{p},E) = \tfrac{1}{2}\{B_0[|\mathbf{p}|,E,(\mathbf{S}_A\cdot\hat{\mathbf{p}})^2] + \boldsymbol{\sigma}\cdot\boldsymbol{\mathcal{F}}_{\mathcal{M}}(\mathbf{p},E)\}, \tag{B2}$$

where $\mathbf{p} = -\mathbf{p}_{\rm mis}$ is the nucleon three-momentum inside the target, the index $\mathcal{M}$ refers to the third component with respect to the quantization axis $\hat{S}_A$, and $\boldsymbol{\mathcal{F}}_{\mathcal{M}}(\mathbf{p},E)$ is a pseudovector depending upon the vector $\hat{\mathbf{p}}$ and the peudovector $\mathbf{S}_A$

$$\boldsymbol{\mathcal{F}}_{\mathcal{M}}(\mathbf{p},E) = \mathbf{S}_A B_{1,\mathcal{M}}[|\mathbf{p}|,E,(\mathbf{S}_A\cdot\hat{\mathbf{p}})^2] + \hat{\mathbf{p}}(\mathbf{S}_A\cdot\hat{\mathbf{p}})B_{2,\mathcal{M}}[|\mathbf{p}|,E,(\mathbf{S}_A\cdot\hat{\mathbf{p}})^2]. \tag{B3}$$

In the case where the FSI is considered through a Glauber operator at high momentum transfer, there is a further dependence of the spectral function upon the vector $\mathbf{q}$ and Eqs. (B2) and (B3) are replaced by

$$\boldsymbol{\mathcal{P}}_{\mathcal{M}}(\mathbf{p},E,\mathbf{q}) = \tfrac{1}{2}\{B_0[|\mathbf{p}|,E,(\mathbf{S}_A\cdot\hat{\mathbf{p}})^2,|\mathbf{q}|,(\mathbf{S}_A\cdot\hat{\mathbf{q}})^2,\hat{\mathbf{p}}\cdot\hat{\mathbf{q}}] + \boldsymbol{\sigma}\cdot\boldsymbol{\mathcal{F}}_{\mathcal{M}}(\mathbf{p},E,\mathbf{q})\}, \tag{B4}$$

$$\begin{aligned}\boldsymbol{\mathcal{F}}_{\mathcal{M}}(\mathbf{p},E,\mathbf{q}) = {}& \mathbf{S}_A B_{1,\mathcal{M}}[|\mathbf{p}|,E,(\mathbf{S}_A\cdot\hat{\mathbf{p}})^2,|\mathbf{q}|,(\mathbf{S}_A\cdot\hat{\mathbf{q}})^2,\hat{\mathbf{p}}\cdot\hat{\mathbf{q}}] + \hat{\mathbf{p}}(\mathbf{S}_A\cdot\hat{\mathbf{p}})B_{2,\mathcal{M}}[|\mathbf{p}|,E,(\mathbf{S}_A\cdot\hat{\mathbf{p}})^2,|\mathbf{q}|,(\mathbf{S}_A\cdot\hat{\mathbf{q}})^2,\hat{\mathbf{p}}\cdot\hat{\mathbf{q}}]\\ &+ \hat{\mathbf{p}}(\mathbf{S}_A\cdot\hat{\mathbf{q}})B_{3,\mathcal{M}}[|\mathbf{p}|,E,(\mathbf{S}_A\cdot\hat{\mathbf{p}})^2,|\mathbf{q}|,(\mathbf{S}_A\cdot\hat{\mathbf{q}})^2,\hat{\mathbf{p}}\cdot\hat{\mathbf{q}}] + \hat{\mathbf{q}}(\mathbf{S}_A\cdot\hat{\mathbf{p}})B_{4,\mathcal{M}}[|\mathbf{p}|,E,(\mathbf{S}_A\cdot\hat{\mathbf{p}})^2,|\mathbf{q}|,(\mathbf{S}_A\cdot\hat{\mathbf{q}})^2,\hat{\mathbf{p}}\cdot\hat{\mathbf{q}}]\\ &+ \hat{\mathbf{q}}(\mathbf{S}_A\cdot\hat{\mathbf{q}})B_{5,\mathcal{M}}[|\mathbf{p}|,E,(\mathbf{S}_A\cdot\hat{\mathbf{p}})^2,|\mathbf{q}|,(\mathbf{S}_A\cdot\hat{\mathbf{q}})^2,\hat{\mathbf{p}}\cdot\hat{\mathbf{q}}] + \hat{\mathbf{p}}\mathrm{x}\hat{\mathbf{q}}B_{6,\mathcal{M}}[|\mathbf{p}|,E,(\mathbf{S}_A\cdot\hat{\mathbf{p}})^2,|\mathbf{q}|,(\mathbf{S}_A\cdot\hat{\mathbf{q}})^2,\hat{\mathbf{p}}\cdot\hat{\mathbf{q}}].\end{aligned} \tag{B5}$$

The above expressions for the spectral function, put in evidence the dependence upon $\mathbf{S}_A$, as well as the dependence of the scalar functions $B_i$ $(i = 1,\ldots,6)$ by the possible scalars $|\mathbf{p}|,E,(\mathbf{S}_A\cdot\hat{\mathbf{p}})^2,|\mathbf{q}|,(\mathbf{S}_A\cdot\hat{\mathbf{q}})^2,\hat{\mathbf{p}}\cdot\hat{\mathbf{q}}$. If $\mathbf{S}_A$ is orthogonal to the $z$ axis, $\boldsymbol{\mathcal{F}}_{\mathcal{M}}(\mathbf{p},E,\mathbf{q})$ reduces to

$$\begin{aligned}\boldsymbol{\mathcal{F}}_{\mathcal{M}}(\mathbf{p},E,\mathbf{q}) = {}& \mathbf{S}_A B_{1,\mathcal{M}}[|\mathbf{p}|,E,(\mathbf{S}_A\cdot\hat{\mathbf{p}})^2,|\mathbf{q}|,\hat{\mathbf{p}}\cdot\hat{\mathbf{q}}] + \hat{\mathbf{p}}(\mathbf{S}_A\cdot\hat{\mathbf{p}})B_{2,\mathcal{M}}[|\mathbf{p}|,E,(\mathbf{S}_A\cdot\hat{\mathbf{p}})^2,|\mathbf{q}|,\hat{\mathbf{p}}\cdot\hat{\mathbf{q}}]\\ &+ \hat{\mathbf{q}}(\mathbf{S}_A\cdot\hat{\mathbf{p}})B_{4,\mathcal{M}}[|\mathbf{p}|,E,(\mathbf{S}_A\cdot\hat{\mathbf{p}})^2,|\mathbf{q}|,\hat{\mathbf{p}}\cdot\hat{\mathbf{q}}] + \hat{\mathbf{p}}\mathrm{x}\hat{\mathbf{q}}B_{6,\mathcal{M}}[|\mathbf{p}|,E,(\mathbf{S}_A\cdot\hat{\mathbf{p}})^2,|\mathbf{q}|,\hat{\mathbf{p}}\cdot\hat{\mathbf{q}}].\end{aligned} \tag{B6}$$

From Eq. (B4) one has

$$B_0[|\mathbf{p}|,E,(\mathbf{S}_A\cdot\hat{\mathbf{p}})^2,|\mathbf{q}|,\hat{\mathbf{p}}\cdot\hat{\mathbf{q}}] = Tr[\boldsymbol{\mathcal{P}}_{\mathcal{M}}(\mathbf{p},E,\mathbf{q})], \tag{B7}$$

$$\boldsymbol{\mathcal{F}}_{\mathcal{M}}(\mathbf{p},E,\mathbf{q}) = Tr[\boldsymbol{\mathcal{P}}_{\mathcal{M}}(\mathbf{p},E,\mathbf{q})\boldsymbol{\sigma}]. \tag{B8}$$

Let us now express the distorted spectral function with a polarization axis along $\mathbf{S}_A$ [cf. Eqs. (42) and (43)] in terms of the components given in Eq. (49), that correspond to a polarization axis along $\hat{q}$ by using Eq. (B1). Since we are interested in a transversely polarized target, i.e., $\mathbf{S}_A \equiv \{1,0,0\}$, one has to consider $\beta = 90^\circ$, and the components of the spectral functions are

$$\mathcal{P}_{\mathcal{M}=\frac{1}{2},\sigma\sigma'}(\mathbf{p},E,\mathbf{q}) = \tfrac{1}{2}\left\{\mathcal{P}^{\frac{1}{2}\frac{1}{2}}_{\sigma\sigma'}(\mathbf{p},E,\mathbf{q}) + \mathcal{P}^{-\frac{1}{2}-\frac{1}{2}}_{\sigma\sigma'}(\mathbf{p},E,\mathbf{q}) + \left[\mathcal{P}^{\frac{1}{2}-\frac{1}{2}}_{\sigma\sigma'}(\mathbf{p},E,\mathbf{q}) + \mathcal{P}^{-\frac{1}{2}\frac{1}{2}}_{\sigma\sigma'}(\mathbf{p},E,\mathbf{q})\right]\right\}. \tag{B9}$$

If the nucleus is polarized along $-\mathbf{S}_A$, the state of the nucleus can be written as follows:

$$\left|\frac{1}{2},-\frac{1}{2}\right\rangle_{\hat{S}_A} = -\sin\frac{\beta}{2}\left|\frac{1}{2},\frac{1}{2}\right\rangle_{\hat{q}} + \cos\frac{\beta}{2}\left|\frac{1}{2},-\frac{1}{2}\right\rangle_{\hat{q}} \tag{B10}$$

and the spectral function becomes

$$\mathcal{P}_{\mathcal{M}=-\frac{1}{2},\sigma\sigma'}(\mathbf{p},E,\mathbf{q}) = \tfrac{1}{2}\left\{\mathcal{P}^{\frac{1}{2}\frac{1}{2}}_{\sigma\sigma'}(\mathbf{p},E,\mathbf{q}) + \mathcal{P}^{-\frac{1}{2}-\frac{1}{2}}_{\sigma\sigma'}(\mathbf{p},E,\mathbf{q}) - \left[\mathcal{P}^{\frac{1}{2}-\frac{1}{2}}_{\sigma\sigma'}(\mathbf{p},E,\mathbf{q}) + \mathcal{P}^{-\frac{1}{2}\frac{1}{2}}_{\sigma\sigma'}(\mathbf{p},E,\mathbf{q})\right]\right\}. \tag{B11}$$

To obtain the real and the imaginary parts of the quantity $[\mathcal{P}^{N\,\frac{1}{2}-\frac{1}{2}}_{\frac{1}{2}-\frac{1}{2}}(E,\mathbf{p}_{\rm mis}) + \mathcal{P}^{N\,-\frac{1}{2}\frac{1}{2}}_{\frac{1}{2}-\frac{1}{2}}(E,\mathbf{p}_{\rm mis})]$, needed to evaluate the single spin asymmetries [see Eq. (61)], let us first consider the $x$ and the $y$ components of $\boldsymbol{\mathcal{F}}_{\frac{1}{2}}(\mathbf{p},E,\mathbf{q})$ with $\mathbf{S}_A = \mathbf{S}_3$ along the $x$ axis.

From Eq. (B6), one has

$$\begin{aligned}\mathcal{F}^{\hat{x}}_{\frac{1}{2}x}(\mathbf{p},E,\mathbf{q}) = {}& B_{1,\frac{1}{2}}[|\mathbf{p}|,E,(\mathbf{S}_A\cdot\hat{\mathbf{p}})^2,|\mathbf{q}|,\hat{\mathbf{p}}\cdot\hat{\mathbf{q}}] + \sin^2\theta\cos^2\phi B_{2,\frac{1}{2}}[|\mathbf{p}|,E,(\mathbf{S}_A\cdot\hat{\mathbf{p}})^2,|\mathbf{q}|,\hat{\mathbf{p}}\cdot\hat{\mathbf{q}}]\\ &+ \sin\theta\sin\phi B_{6,\frac{1}{2}}[|\mathbf{p}|,E,(\mathbf{S}_A\cdot\hat{\mathbf{p}})^2,|\mathbf{q}|,\hat{\mathbf{p}}\cdot\hat{\mathbf{q}}],\end{aligned} \tag{B12}$$

$$\mathcal{F}^{\hat{x}}_{\frac{1}{2}y}(\mathbf{p},E,\mathbf{q}) = \sin^2\theta\cos\phi\sin\phi B_{2,\frac{1}{2}}[|\mathbf{p}|,E,(\mathbf{S}_A\cdot\hat{\mathbf{p}})^2,|\mathbf{q}|,\hat{\mathbf{p}}\cdot\hat{\mathbf{q}}] - \sin\theta\cos\phi B_{6,\frac{1}{2}}[|\mathbf{p}|,E,(\mathbf{S}_A\cdot\hat{\mathbf{p}})^2,|\mathbf{q}|,\hat{\mathbf{p}}\cdot\hat{\mathbf{q}}], \tag{B13}$$

where the angles $\theta$ and $\phi$ define the direction of the nucleon momentum $\boldsymbol{p}$. From Eq. (B8) and Eq. (B9), one obtains

$$\mathcal{F}^{\hat{x}}_{\frac{1}{2}x}(\mathbf{p},E,\mathbf{q}) = \mathrm{Tr}[\mathcal{P}_{\mathcal{M}=\frac{1}{2}}(\mathbf{p},E,\mathbf{q})\sigma_x] = \mathrm{Re}\big[\mathcal{P}^{\frac{1}{2}\frac{1}{2}}_{\frac{1}{2}-\frac{1}{2}}(\mathbf{p},E,\mathbf{q}) + \mathcal{P}^{-\frac{1}{2}-\frac{1}{2}}_{\frac{1}{2}-\frac{1}{2}}(\mathbf{p},E,\mathbf{q}) + \mathcal{P}^{\frac{1}{2}-\frac{1}{2}}_{\frac{1}{2}-\frac{1}{2}}(\mathbf{p},E,\mathbf{q}) + \mathcal{P}^{-\frac{1}{2}\frac{1}{2}}_{\frac{1}{2}-\frac{1}{2}}(\mathbf{p},E,\mathbf{q})\big], \tag{B14}$$

$$\mathcal{F}^{\hat{x}}_{\frac{1}{2}y}(\mathbf{p},E,\mathbf{q}) = \mathrm{Tr}[\mathcal{P}_{\mathcal{M}=\frac{1}{2}}(\mathbf{p},E,\mathbf{q})\sigma_y] = -\mathrm{Im}\big[\mathcal{P}^{\frac{1}{2}\frac{1}{2}}_{\frac{1}{2}-\frac{1}{2}}(\mathbf{p},E,\mathbf{q}) + \mathcal{P}^{-\frac{1}{2}-\frac{1}{2}}_{\frac{1}{2}-\frac{1}{2}}(\mathbf{p},E,\mathbf{q}) + \mathcal{P}^{\frac{1}{2}-\frac{1}{2}}_{\frac{1}{2}-\frac{1}{2}}(\mathbf{p},E,\mathbf{q}) + \mathcal{P}^{-\frac{1}{2}\frac{1}{2}}_{\frac{1}{2}-\frac{1}{2}}(\mathbf{p},E,\mathbf{q})\big]. \tag{B15}$$

Then let us consider the $x$ and the $y$ components of $\boldsymbol{\mathcal{F}}_{\frac{1}{2}}(\mathbf{p},E,\mathbf{q})$ with $\mathbf{S}_3$ opposite to the $x$ axis. From Eq. (B6), one has

$$\begin{aligned}\mathcal{F}^{-\hat{x}}_{\frac{1}{2}x}(\mathbf{p},E,\mathbf{q}) = &-B_{1,\frac{1}{2}}[|\mathbf{p}|,E,(\mathbf{S}_A\cdot\hat{\mathbf{p}})^2,|\mathbf{q}|,\hat{\mathbf{p}}\cdot\hat{\mathbf{q}}] - \sin^2\theta\cos^2\phi B_{2,\frac{1}{2}}[|\mathbf{p}|,E,(\mathbf{S}_A\cdot\hat{\mathbf{p}})^2,|\mathbf{q}|,\hat{\mathbf{p}}\cdot\hat{\mathbf{q}}]\\ &+ \sin\theta\sin\phi B_{6,\frac{1}{2}}[|\mathbf{p}|,E,(\mathbf{S}_A\cdot\hat{\mathbf{p}})^2,|\mathbf{q}|,\hat{\mathbf{p}}\cdot\hat{\mathbf{q}}],\end{aligned} \tag{B16}$$

$$\mathcal{F}^{-\hat{x}}_{\frac{1}{2}y}(\mathbf{p},E,,\mathbf{q}) = -\sin^2\theta\cos\phi\sin\phi B_{2,\frac{1}{2}}[|\mathbf{p}|,E,(\mathbf{S}_A\cdot\hat{\mathbf{p}})^2,|\mathbf{q}|,\hat{\mathbf{p}}\cdot\hat{\mathbf{q}}] - \sin\theta\cos\phi B_{6,\frac{1}{2}}[|\mathbf{p}|,E,(\mathbf{S}_A\cdot\hat{\mathbf{p}})^2,|\mathbf{q}|,\hat{\mathbf{p}}\cdot\hat{\mathbf{q}}], \tag{B17}$$

while from Eqs. (B8) and (B11) one obtains

$$\mathcal{F}^{-\hat{x}}_{\frac{1}{2}x}(\mathbf{p},E,\mathbf{q}) = \mathrm{Tr}[\mathcal{P}_{\mathcal{M}=-\frac{1}{2}}(\mathbf{p},E,\mathbf{q})\sigma_x] = \mathrm{Re}\big[\mathcal{P}^{\frac{1}{2}\frac{1}{2}}_{\frac{1}{2}-\frac{1}{2}}(\mathbf{p},E,\mathbf{q}) + \mathcal{P}^{-\frac{1}{2}-\frac{1}{2}}_{\frac{1}{2}-\frac{1}{2}}(\mathbf{p},E,\mathbf{q}) - \mathcal{P}^{\frac{1}{2}-\frac{1}{2}}_{\frac{1}{2}-\frac{1}{2}}(\mathbf{p},E,\mathbf{q}) - \mathcal{P}^{-\frac{1}{2}\frac{1}{2}}_{\frac{1}{2}-\frac{1}{2}}(\mathbf{p},E,\mathbf{q})\big], \tag{B18}$$

$$\mathcal{F}^{-\hat{x}}_{\frac{1}{2}y}(\mathbf{p},E,\mathbf{q}) = \mathrm{Tr}[\mathcal{P}_{\mathcal{M}=-\frac{1}{2}}(\mathbf{p},E,\mathbf{q})\sigma_y] = -\mathrm{Im}\big[\mathcal{P}^{\frac{1}{2}\frac{1}{2}}_{\frac{1}{2}-\frac{1}{2}}(\mathbf{p},E,\mathbf{q}) + \mathcal{P}^{-\frac{1}{2}-\frac{1}{2}}_{\frac{1}{2}-\frac{1}{2}}(\mathbf{p},E,\mathbf{q}) - \mathcal{P}^{\frac{1}{2}-\frac{1}{2}}_{\frac{1}{2}-\frac{1}{2}}(\mathbf{p},E,\mathbf{q}) - \mathcal{P}^{-\frac{1}{2}\frac{1}{2}}_{\frac{1}{2}-\frac{1}{2}}(\mathbf{p},E),\mathbf{q}\big]. \tag{B19}$$

The difference of Eqs. (B12) and (B16) is equal to the difference of Eqs. (B14) and (B18),

$$2B_{1,\frac{1}{2}}[|\mathbf{p}|,E,(\mathbf{S}_A\cdot\hat{\mathbf{p}})^2,|\mathbf{q}|,\hat{\mathbf{p}}\cdot\hat{\mathbf{q}}] + 2\sin^2\theta\cos^2\phi B_{2,\frac{1}{2}}[|\mathbf{p}|,E,(\mathbf{S}_A\cdot\hat{\mathbf{p}})^2,|\mathbf{q}|,\hat{\mathbf{p}}\cdot\hat{\mathbf{q}}] = 2\mathrm{Re}\big[\mathcal{P}^{\frac{1}{2}-\frac{1}{2}}_{\frac{1}{2}-\frac{1}{2}}(\mathbf{p},E,\mathbf{q}) + \mathcal{P}^{-\frac{1}{2}\frac{1}{2}}_{\frac{1}{2}-\frac{1}{2}}(\mathbf{p},E,\mathbf{q})\big], \tag{B20}$$

and the difference of Eqs. (B13) and (B17) is equal to the difference of Eqs. (B15) and (B19),

$$2\sin^2\theta\cos\phi\sin\phi B_{2,\frac{1}{2}}[|\mathbf{p}|,E,(\mathbf{S}_A\cdot\hat{\mathbf{p}})^2,|\mathbf{q}|,\hat{\mathbf{p}}\cdot\hat{\mathbf{q}}] = -2\mathrm{Im}\big[\mathcal{P}^{\frac{1}{2}-\frac{1}{2}}_{\frac{1}{2}-\frac{1}{2}}(\mathbf{p},E,\mathbf{q}) + \mathcal{P}^{-\frac{1}{2}\frac{1}{2}}_{\frac{1}{2}-\frac{1}{2}}(\mathbf{p},E,\mathbf{q})\big]. \tag{B21}$$

Let us stress that the scalar functions $B_1$ and $B_2$ do depend on the variable $\phi$ only through $(\mathbf{S}_A\cdot\hat{\mathbf{p}})^2 = (\sin\theta\cos\phi)^2$, since $\hat{\mathbf{p}}\cdot\hat{\mathbf{q}} = \cos\theta$.

In the nucleon tensor operators $\hat{w}^{sN}_{\mu\nu}$ that give rise to the Collins and the Sivers effect, the nucleon momentum can appear directly or through the nucleon spin operator. Therefore, terms of zero order in $\boldsymbol{p}_\perp/m_N$ can appear, as well as terms of the first, second, and third orders ($\perp$ means orthogonal to the $\hat{q} = \hat{z}$ axis) [3]. Once multiplied by the spectral function and integrated over the nucleon momentum, the terms of the second and third orders can be discarded, since the spectral function decreases rapidly as a function of the nucleon momentum (see, e.g., Fig. 2).

In the imaginary part, $\mathrm{Im}[w^{sN\frac{1}{2}-\frac{1}{2}}_{\mu\nu}]$, the terms of zero order and of the first order in $\boldsymbol{p}_\perp/m_N$, once multiplied by the left-hand side of Eq. (B21) and integrated over $\phi$, do not give contribution to the hadronic tensor, since one has to integrate quantities like $(\cos\phi\sin\phi)$, $(\cos^2\phi\sin\phi)$, or $(\cos\phi\sin^2\phi)$ times a function of $\cos^2\phi$. Then the product of the imaginary quantities in Eq. (60) does not give contribution to the cross section.

An analogous analysis can be performed on the real part $\mathrm{Re}[w^{sN\frac{1}{2}-\frac{1}{2}}_{\mu\nu}]$ of the nucleon tensor. In this case, the terms of zero order in $\boldsymbol{p}_\perp$ give a nonzero contribution, while the first-order terms yield zero, once the integration over $\phi$ is performed.

Let us finally notice that since the transverse components of $\mathbf{p}$ can be disregarded, as discussed above, the expressions for $\Delta\sigma^N_{Col}$ and for $\Delta\sigma^N_{Siv}$ of Eqs. (66) and (67) of our paper, that were obtained in a reference frame where $\boldsymbol{p}_\perp = 0$ (see, e.g., Eqs. (6.5.18) and (6.5.17) of Ref. [3]), can be safely used.

[1] J. J. Aubert, G. Bassompierre, K. H. Becks, C. Best, E. Boehm, X. de Bouard, F. W. Brasse, C. Broll, S. Brown, J. Carr *et al.* (European Muon Collaboration), Phys. Lett. B **123**, 275 (1983).

[2] J. Ashman, B. Badelek, G. Baum, J. Beaufays, C. P. Bee, C. Benchouk, I. G. Bird, S. C. Brown, M. C. Caputo, H. W. K. Cheung *et al.* (European Muon Collaboration), Phys. Lett. B **206**, 364 (1988).

[3] V. Barone, A. Drago, and P. G. Ratcliffe, Phys. Rept. **359**, 1 (2002).

[4] V. Barone, F. Bradamante, and A. Martin, Prog. Part. Nucl. Phys. **65**, 267 (2010).

[5] J. Beringer, J.-F. Arguin, R. M. Barnett, K. Copic, O. Dahl, D. E. Groom, C.-J. Lin, J. Lys, H. Murayama, C. G. Wohl *et al.* (Particle Data Group Collaboration), Phys. Rev. D **86**, 010001 (2012).

[6] S. E. Kuhn, J.-P. Chen, and E. Leader, Prog. Part. Nucl. Phys. **63**, 1 (2009).

[7] M. Arneodo, Phys. Rept. **240**, 301 (1994).

[8] G. Piller and W. Weise, Phys. Rept. **330**, 1 (2000).

[9] O. Hen, D. W. Higinbotham, G. A. Miller, E. Piasetzky, and L. B. Weinstein, Int. J. Mod. Phys. E **22**, 1330017 (2013).

[10] M. Diehl, Eur. Phys. J. A **52**, 149 (2016).

[11] R. Dupré and S. Scopetta, Eur. Phys. J. A **52**, 159 (2016).

[12] D. W. Sivers, Phys. Rev. D **41**, 83 (1990); **43**, 261 (1991).

[13] D. Boer and P. J. Mulders, Phys. Rev. D **57**, 5780 (1998).

[14] U. D'Alesio and F. Murgia, Prog. Part. Nucl. Phys. **61**, 394 (2007).

[15] C. Ciofi degli Atti, S. Scopetta, E. Pace, and G. Salmè, Phys. Rev. C **48**, R968(R) (1993).

[16] K. Abe, T. Akagi, B. D. Anderson, P. L. Anthony, R. G. Arnold, T. Averett, H. R. Band, C. M. Berisso, P. Bogorad, H. Borel *et al.* (E154 Collaboration), Phys. Rev. Lett. **79**, 26 (1997).

[17] C. Ciofi degli Atti, E. Pace, and G. Salmè, Phys. Rev. C **46**, R1591(R) (1992).

[18] R.-W. Schulze and P. U. Sauer, Phys. Rev. C **48**, 38 (1993).

[19] C. Ciofi degli Atti, E. Pace, and G. Salmè, Phys. Rev. C **51**, 1108 (1995).

[20] A. Kievsky, E. Pace, G. Salmè, and M. Viviani, Phys. Rev. C **56**, 64 (1997).

[21] L. P. Kaptari, A. Yu. Umnikov, C. Ciofi degli Atti, S. Scopetta and K. Yu. Kazakov, Phys. Rev. C **51**, 52 (1995).

[22] C. Ciofi degli Atti and S. Scopetta, Phys. Lett. B **404**, 223 (1997).

[23] G. Cates, H. Baghdasaryan, D. Day, P. Dolph, N. Kalantarians, R. Lindgren, N. Liyanage, V. Nelyubin, Al Tobias, E. Cisbani *et al.*, JLAB approved experiment E12-09-018, Measurement of Semi-Inclusive Pion and Kaon electroproduction in the DIS Regime on a Transversely Polarized $^3$He Target using the Super BigBite and BigBite Spectrometers in Hall A, http://hallaweb.jlab.org/collab/PAC/PAC38/E12-09-018-SIDIS.pdf (unpublished); X. Jiang, A. Afanasev, K. Allada, J. Annand, T. Averett, F. Benmokhtar, W. Bertozzi, F. Butaru, G. Cates, C. Chang *et al.*, Experiment PR12-09-014: Measurement of Single Target-Spin Asymmetry in Semi-Inclusive n (e,e'$\pi$) Reaction on a Transversely Polarized $^3$He Target, www.jlab.org/exp_prog/generated/apphalla.html (unpublished); J. Arrington, R. Dupre, A. El Alaoui, K. Hafidi, R. J. Holt, P. E. Reimer, X. Zhan, A. Kolarkar, X. Qian, K. Aniol *et al.*, Asymmetries in Semi-Inclusive Deep-Inelastic (e,e'$\pi^{\pm}$) Reactions on a Longitudinally Polarized $^3$He Target at 8.8 and 11 GeV, Experiment E12-11-007, www.jlab.org/~jinhuang/12GeV/12GeVLongitudinalHe3.pdf (unpublished).

[24] J. C. Collins, Nucl. Phys. B **396**, 161 (1993).

[25] S. J. Brodsky, D. S. Hwang, and I. Schmidt, Phys. Lett. B **530**, 99 (2002).

[26] A. Airapetian, N. Akopov, Z. Akopov, M. Amarian, A. Andrus, E. C. Aschenauer, W. Augustyniak, R. Avakian, A. Avetissian, E. Avetissian *et al.* (HERMES Collaboration), Phys. Rev. Lett. **94**, 012002 (2005).

[27] V. Y. Alexakhin, Yu. Alexandrov, G. D. Alexeev, A. Amoroso, B. Badelek, F. Balestra, J. Ball, G. Baum, Y. Bedfer, P. Berglund *et al.* (COMPASS Collaboration), Phys. Rev. Lett. **94**, 202002 (2005).

[28] S. J. Brodsky and S. Gardner, Phys. Lett. B **643**, 22 (2006).

[29] X. Qian, K. Allada, C. Dutta, J. Huang, J. Katich, Y. Wang, Y. Zhang, K. Aniol, J. R. M. Annand, T. Averett *et al.* (Jefferson Lab Hall A Collaboration), Phys. Rev. Lett. **107**, 072003 (2011).

[30] H. Gao, L. Gamberg, J.-P. Chen, X. Qian,Y. Qiang, M. Huang, A. Afanasev, M. Anselmino, H. Avakian, G. Cates *et al.*, Eur. Phys. J. Plus **126**, 2 (2011).

[31] S. Scopetta, Phys. Rev. D **75**, 054005 (2007).

[32] R. B. Wiringa, V. G. J. Stoks, and R. Schiavilla, Phys. Rev. C **51**, 38 (1995).

[33] C. Ciofi degli Atti and L. P. Kaptari, Phys. Rev. C **83**, 044602 (2011).

[34] C. Ciofi degli Atti, L. P. Kaptari, and S. Scopetta, Eur. Phys. J. A **5**, 191 (1999).

[35] C. Ciofi degli Atti, L. P. Kaptari, and B. Z. Kopeliovich, Eur. Phys. J. A **19**, 145 (2004).

[36] W. Melnitchouk, M. Sargsian, and M. I. Strikman, Z. Phys. A **359**, 99 (1997).

[37] V. Palli, C. Ciofi degli Atti, L. P. Kaptari, C. B. Mezzetti, and M. Alvioli, Phys. Rev. C **80**, 054610 (2009).

[38] L. P. Kaptari, A. Del Dotto, E. Pace, G. Salmè, and S. Scopetta, Phys. Rev. C **89**, 035206 (2014).

[39] B. D. Anderson, J. Arrington, D. F. Geesaman, K. Hafidi, R. J. Holt, D. Potterveld, P. Reimer, J. Rubin, J. Singh, X. Zhan *et al.*, JLAB approved experiment C12-10-103, Measurement of the F2n/F2p, d/u Ratios and A=3 EMC Effect in Deep Inelastic Electron Scattering Off the Tritium and Helium Mirror Nuclei, http://hallaweb.jlab.org/collab/PAC/PAC37/C12-10-103-Tritium.pdf (unpublished).

[40] P. A. M. Dirac, Rev. Mod. Phys. **21**, 392 (1949).

[41] A. Del Dotto, E. Pace, G. Salmè, and S. Scopetta, Phys. Rev. C **95**, 014001 (2017).

[42] S. Scopetta, A. Del Dotto, L. Kaptari, E. Pace, M. Rinaldi, and G. Salmè, Few Body Syst. **56**, 425 (2015).

[43] E. Pace, A. Del Dotto, L. Kaptari, M. Rinaldi, G. Salmè, and S. Scopetta, Few Body Syst. **57**, 601 (2016).

[44] S. Kuhn, C. Keppel, W. Melnitchouk, G. Dodge, A. Klimenko, S. Stepanyan, L. Weinstein, W. Brooks, C. Ciofi degli Atti, L. Kaptari *et al.*, The structure of the free neutron via spectator tagging, www.jlab.org/exp_prog/proposals/03prop.html (PR03-012.pdf); www.jlab.org/exp_prog/proposals/06/PR12-06-113.pdf (unpublished).

[45] C. Ciofi degli Atti and L. P. Kaptari, Phys. Rev. Lett. **100**, 122301 (2008).

[46] X. Yan, K. Allada, K. Anio, J. R. M. Annand, T. Averett, F. Benmokhtar, W. Bertozzi, P. C. Bradshaw, P. Bosted, A. Camsonne *et al.*, Phys. Rev. C **95**, 035209 (2017).

[47] D. A. Varshalovich, A. N. Moskalev, and V. K. Khersonskii, *Quantum Theory of Angular Momentum* (World Scientific, Singapore, 1988).

[48] A. Bacchetta, U. D'Alesio, M. Diehl, and C. A. Miller, Phys. Rev. D **70**, 117504 (2004).

[49] A. Kievsky, M. Viviani, and S. Rosati, Nucl. Phys. A **577**, 511 (1994), and private communication.

[50] M. Glück, E. Reya, and A. Vogt, Eur. Phys. J. C **5**, 461 (1998).

[51] M. Gluck, E. Reya, M. Stratmann, and W. Vogelsang, Phys. Rev. D **63**, 094005 (2001).
[52] M. Anselmino, M. Boglione, U. D'Alesio, A. Kotzinian, F. Murgia, and A. Prokudin, Phys. Rev. D **72**, 094007 (2005); **72**, 099903(E) (2005).
[53] S. Kretzer, Phys. Rev. D **62**, 054001 (2000).
[54] D. Amrath, A. Bacchetta, and A. Metz, Phys. Rev. D **71**, 114018 (2005).
[55] J. J. Ethier and W. Melnitchouk, Phys. Rev. C **88**, 054001 (2013).
[56] A. Accardi, J. L. Albacete, M. Anselmino, N. Armesto, E. C. Aschenauer, A. Bacchetta, D. Boer, W. K. Brooks, T. Burton, N.-B. Chang *et al.*, Eur. Phys. J. A **52**, 268 (2016).
[57] A. Del Dotto, L. Kaptari, E. Pace, G. Salmè, and S. Scopetta, Few Body Syst. **58**, 23 (2017).
[58] T. L. Trueman, Phys. Rev. D **77**, 054005 (2008).
[59] I. G. Alekseev, A. Bravar, G. Bunce, S. Dhawan, K. O. Eyser, R. Gill, W. Haeberli, H. Huang, O. Jinnouchi, A. Kponou *et al.*, Phys. Rev. D **79**, 094014 (2009).